



Contents lists available at ScienceDirect

Journal of Rock Mechanics and Geotechnical Engineering

journal homepage: www.rockgeotech.org

Full Length Article

A unified critical state model for geomaterials with an application to tunnelling

Hai-Sui Yu ^{a,*}, Pei-Zhi Zhuang ^a, Pin-Qiang Mo ^b^aSchool of Civil Engineering, University of Leeds, Leeds, LS2 9JT, UK^bState Key Laboratory for GeoMechanics and Deep Underground Engineering, China University of Mining and Technology, Xuzhou, 221116, Jiangsu, China

ARTICLE INFO

Article history:

Received 11 August 2018

Received in revised form

1 September 2018

Accepted 4 September 2018

Available online 13 December 2018

Keywords:

Critical state soil mechanics

Constitutive models

Cavity contraction

Tunnelling in soil

ABSTRACT

This paper is prepared in honour of Professor E.T. Brown for his outstanding contributions to rock mechanics and geotechnical engineering and also for his personal influence on the first author's research career in geomechanics and geotechnical engineering. As a result, we have picked a topic that reflects two key research areas in which Professor E.T. Brown has made seminal contributions over a long and distinguished career. These two areas are concerned with the application of the critical state concept to modelling geomaterials and the analysis of underground excavation or tunnelling in geomaterials. Partially due to Professor Brown's influence, the first author has also been conducting research in these two areas over many years. In particular, this paper aims to describe briefly the development of a unified critical state model for geomaterials together with an application to cavity contraction problems and tunnelling in soils.

© 2019 Institute of Rock and Soil Mechanics, Chinese Academy of Sciences. Production and hosting by Elsevier B.V. This is an open access article under the CC BY-NC-ND license (<http://creativecommons.org/licenses/by-nc-nd/4.0/>).

1. Introduction

The critical state theory was first used to develop plasticity models for soils over 60 years ago (Drucker et al., 1957; Roscoe et al., 1958; Roscoe and Schofield, 1963; Roscoe and Burland, 1968; Schofield and Wroth, 1968). Since then, elasto-plastic models based on the critical state concept have been successfully used to describe many important features of soil behaviour. The original Cam-clay (OCC) model was developed by Roscoe and Schofield (1963). Later, Roscoe and Burland (1968) proposed a modified Cam-clay (MCC) model and its generalisation to three-dimensional (3D) stress states. It is now widely accepted that the development of critical state-based constitutive models represents a most important advance in the application of plasticity theory to geotechnical engineering.

The kernel of critical state soil mechanics is that soil and other granular materials, if continuously being sheared and distorted, will ultimately reach a state in which the soil behaves as a frictional fluid with a constant volume and a constant ratio of shear stress to

mean normal stress, regardless of the initial state of the material. This ultimate state was termed the critical state by Roscoe et al. (1958) and Parry (1956, 1958). This fundamental concept of critical states was initially developed based on limited triaxial test data obtained on the reconstituted clay (Parry, 1958; Roscoe et al., 1958; Roscoe and Burland, 1968; Schofield and Wroth, 1968). Over the last few decades, many additional experimental results for a variety of other types of soils and granular materials (e.g. sand, rock, natural clay and other bonded geomaterials, unsaturated soil) have been obtained. They generally confirm, at least to a large extent, the validity of the general concept of critical states (e.g. Atkinson and Bransby, 1977; Been and Jefferies, 1985; Brown and Yu, 1988; Alonso et al., 1990; Leroueil and Vaughan, 1990; Wood, 1990; Allman and Atkinson, 1992; Novello and Johnston, 1995; Klotz and Coop, 2002; Cuss et al., 2003; Toll and Ong, 2003; Yu et al., 2005; Rutter and Glover, 2012; Ali Rahman et al., 2018).

The critical state proves to be a powerful reference state for developing a large number of constitutive models to predict mechanical behaviour of soils when subjected to various loading conditions (Schofield and Wroth, 1968; Wood, 1990; Yu, 2006). As mentioned above, the early development of the critical state soil mechanics was largely based on experimental results of clays. Its extension to sand has been slow and in fact it had not made much progress until the 1980s partly due to the difficulties in determining critical state lines (CSLs) in the laboratory (Wroth and Bassett, 1965;

* Corresponding author.

E-mail addresses: H.Yu@leeds.ac.uk (H.-S. Yu), P.zhuang@leeds.ac.uk (P.-Z. Zhuang), Pinqiang.mo@cumt.edu.cn (P.-Q. Mo).

Peer review under responsibility of Institute of Rock and Soil Mechanics, Chinese Academy of Sciences.

Vesic and Clough, 1968; Been and Jefferies, 1985; Been et al., 1991; Coop and Atkinson, 1993; Klotz and Coop, 2002). Meanwhile, based on a large number of triaxial tests on sand, Been et al. (1991) reported that the critical state concept initially developed in the UK is practically similar to the steady state concept that was developed primarily for earthquake liquefaction applications in sand (Castro, 1969; Castro and Poulos, 1977; Poulos, 1981). This observation seems to be supported by other studies (e.g. Verdugo and Ishihara, 1996; Jefferies and Been, 2006). With reference to the unique critical state, Wroth and Bassett (1965) and Been and Jefferies (1985) proposed to use a state parameter to characterise the state of a sand. It has been shown that many essential soil properties correlate very well with the initial state parameter which is easily measurable in the laboratory (Huang and Yu, 2017). Therefore the state parameter has often been used as a simple model parameter in the constitutive modelling of soils (Collins et al., 1992; Jefferies, 1993; Yu, 1994, 1998; Yang and Li, 2004).

Although the OCC and MCC models prove to be successful for modelling normally consolidated clays, they are unable to predict many important features of the observed behaviour of sands and overconsolidated clays (Schofield and Wroth, 1968; Zienkiewicz and Naylor, 1973; Pender, 1978; Nova and Wood, 1979; Sladen et al., 1985; Jefferies, 1993; Yu, 1998). To further extend the applicability of the critical state concept to sand, overconsolidated clay and other soils, a large number of modifications and generalisations of the standard Cam-clay models have been proposed within the framework of critical state soil mechanics over the last several decades (Gens and Potts, 1988; Yu, 2006). For example, some of these modifications are concerned with the following topics: (a) yield surfaces for heavily overconsolidated clays (e.g. Zienkiewicz and Naylor, 1973; Atkinson and Bransby, 1977; Mita et al., 2004); (b) the critical state modelling of sand behaviour (e.g. Nova and Wood, 1979; Jefferies, 1993); (c) anisotropic yield surfaces for one-dimensionally consolidated soils (e.g. Ohta and Wroth, 1976; Dafalias, 1986; Whittle, 1993); (d) inclusion of plastic deformation within the main yield surface for soils subject to cyclic loading (e.g. Pender, 1978; Carter et al., 1979; Dafalias and Herrmann, 1982; Naylor, 1985); (e) 3D critical state model formulations (e.g. Roscoe and Burland, 1968; Zienkiewicz and Pande, 1977); (f) modelling of rate-dependent behaviour of clays (e.g. Borja and Kavazanjian, 1985; Kutter and Sathialingam, 1992); and (g) considering the inter-particle bonding effect in modelling natural or artificially cemented soil (e.g. Gens and Nova, 1993; Liu and Carter, 2002).

Nevertheless, one common problem had remained for many years and that was related to the use and ability of any single yield surface to predict the behaviour of both clay and sand. To overcome this problem, Yu (1995, 1998) proposed a unified critical state model for both clay and sand, CASM (clay and sand model), based on the state parameter and spacing ratio concepts with a non-associated flow rule. As summarised by Yu et al. (2005), the main novel features of CASM include:

- (a) CASM is of a unified nature: only a single set of yield and plastic potential functions (non-associated) is needed to model the behaviour of both clay and sand under both drained and undrained loading conditions. Many existing models are applicable for either clay or sand, but not for both materials. This is not convenient from the application point of view.
- (b) CASM is relatively simple and therefore can be easily applied in practise. Only two additional material constants with clear physical meaning are introduced compared to the OCC or MCC models, which can be recovered (or approximated) simply by choosing certain values of the new material constants.
- (c) CASM incorporates the well-accepted state parameter concept within the consistent framework of critical state soil

mechanics. The state parameter proves to be of fundamental importance in modelling the behaviour of sands and overconsolidated clays. The CASM represents one of the first attempts to reformulate the standard Cam-clay models in terms of the state parameter.

Although other unified clay and sand models have since appeared, some of the inherent advantages of CASM mentioned above still remain very attractive. For example, the MIT-S1 model proposed by Pestana and Whittle (1999) is much more complex and requires many more model constants; the model developed by Yao et al. (2008) adopted an associated flow rule which is not necessarily suitable for characterising both clay and sand.

The philosophy adopted in developing CASM is that simplicity should be paramount and that the material constants required by the constitutive model should be related to easily measurable and possibly conventional constants (Yu, 1998). Inevitably, some features of clay and sand would not be modelled realistically using CASM. In the past two decades, a number of extensions of CASM to more general cases or to particular types of soil have been carried out by Yu and his co-workers (Sheng et al., 2000; Khong, 2004; Yu et al., 2005, 2007a,b; Yu, 2006; Hu, 2015), and also by other researchers (Khalili et al., 2005; Gonzalez et al., 2009; Zhou and Ng, 2015).

The objective of this paper is to present the unified critical state model, CASM, with an application to cavity contraction problems and tunnelling in clay and sand. The paper is arranged as follows: First of all, the basic formulations of the unified critical state model CASM are summarised in Section 2. Secondly, by using CASM to model soil behaviour, semi-analytical stress and displacement solutions for cavity contraction problems in soils under both drained and undrained conditions are derived and presented in Section 3. Thirdly, the newly derived cavity contraction solutions are applied to estimating the ground response curves and displacements of tunnels in soil in Section 4. Finally, some concluding remarks are made in the final section.

2. A unified critical state model for clay and sand – CASM

Following Schofield and Wroth (1968), the critical state of soil is assumed to be fully defined by Eqs. (1) and (2).

$$q = Mp' \quad (1)$$

$$v = \Gamma - \lambda \ln p' \quad (2)$$

where q and p' denote the deviatoric and mean effective stresses, respectively; $v = 1 + e$ is the specific volume; M is the slope of the CSL in the p' - q space. The parameters Γ , λ , and κ are the well-known critical state constants defined in Fig. 1; v_0 represents its initial value; e is the void ratio; $v_{cs} = \Gamma$ for $p' = 1$ kPa. λ and κ are the slope of the reference consolidation line and that of the unloading-reloading line in the v - $\ln p'$ space, respectively.

In critical state soil mechanics, soil loading history and its current state can be represented by its relative position from the CSL in the v - $\ln p'$ space. A simple measure of this relative position would be the vertical distance in the specific volume from the current state to the CSL. This quantity has been termed as 'the state parameter' ξ (Been and Jefferies, 1985; Yu, 1998). The material behaviour prior to the achievement of the critical state is assumed to be controlled by the state parameter, which is defined mathematically by

$$\xi = v + \lambda \ln p' - \Gamma \quad (3)$$

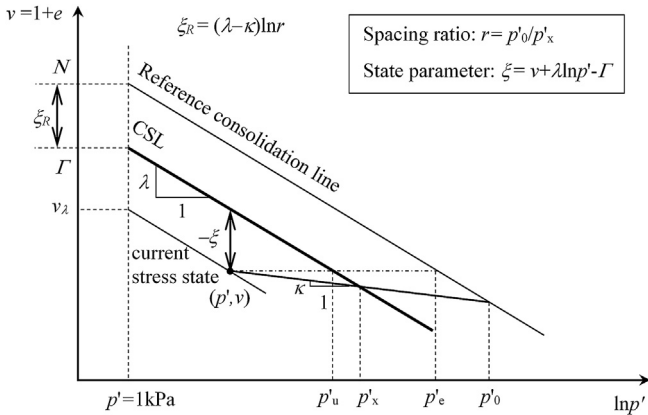


Fig. 1. Definitions of state parameter, critical state constants, and reference state parameters (after Yu, 1998).

It is easily noted that the state parameter ξ is equal to zero at the critical state, positive on the ‘wet’ (or loose) side, and negative on the ‘dry’ (or dense) side.

2.1. State boundary surface and yield function

To illustrate the connections and differences of CASM with the standard Cam-clay models, the state boundary surfaces and yield functions defined in the OCC and MCC models are described briefly here. As presented in the references of Schofield and Wroth (1968) and Roscoe and Burland (1968), their state boundary surfaces are given, respectively, as

$$\frac{q}{Mp'} = \frac{\Gamma + \lambda - \kappa - v - \lambda \ln p'}{\lambda - \kappa} \quad (\text{OCC}) \quad (4)$$

$$\left(\frac{q}{Mp'}\right)^2 = \exp\left(\frac{N - v - \lambda \ln p'}{\lambda - \kappa}\right) - 1 \quad (\text{MCC}) \quad (5)$$

where N is the specific volume at $p' = 1\text{kPa}$ on the reference consolidation line as depicted in Fig. 1.

It is known that Eqs. (4) and (5) are used as the yield functions in the OCC and MCC models, respectively. By using the state parameter of Eq. (3), Yu (1998) noted that the state boundary surfaces of Eqs. (4) and (5) can be expressed, alternatively, as a simpler relationship between the stress ratio and the state parameter, namely:

$$\frac{\eta}{M} = 1 - \frac{\xi}{\xi_R} \quad (\text{OCC}) \quad (6)$$

$$\left(\frac{\eta}{M}\right)^2 = 2^{1-\xi/\xi_R} - 1 \quad (\text{MCC}) \quad (7)$$

where $\eta = |q/p'|$ is known as the stress ratio; and ξ_R is a positive reference state parameter, which denotes the vertical distance between the CSL and a reference consolidation line (RCL). As shown in Fig. 1, the reference consolidation line is assumed to be parallel to the CSL. For clays, the isotropic consolidation line, NCL, is used as the reference consolidation line. In the OCC model, the reference state parameter is $\xi_R = (\lambda - \kappa) \ln r = (\lambda - \kappa) \ln e = \lambda - \kappa$, where r is known as the spacing ratio (Wroth and Houslyby, 1985; Yu, 1998). For sands, information about the NCL may not be easily measured and in such a case, the reference state parameter may be chosen as the loosest state that a soil is likely to reach in practise. When a soil is yielding, the stress-state relation of the OCC model (i.e. Eq. (6)) implies that the stress ratio η increases linearly with a decrease in

the state parameter, and a nonlinear relation is defined in the MCC model as given by Eq. (7), see Fig. 2a.

Based on a detailed study of the experimental state boundary surfaces as reported by Stroud (1971), Lee and Seed (1967), Schofield and Wroth (1968), Atkinson and Bransby (1977), Sladen et al. (1985), Coop and Lee (1993), and Yu (1995, 1998) proposed the use of a general stress–state relationship to describe the state boundary surface for a variety of soils:

$$\left(\frac{\eta}{M}\right)^n = 1 - \frac{\xi}{\xi_R} \quad (8)$$

where n is a new material constant. Example state boundary surfaces defined by Eq. (8) is shown in Fig. 2b.

From Fig. 1, it can be shown that

$$\frac{\xi}{\xi_R} = \frac{-(\lambda - \kappa) \ln(p'_x/p')}{(\lambda - \kappa) \ln r} = 1 + \frac{\ln(p'/p'_0)}{\ln r} \quad (9)$$

where p'_x is the mean effective stress at the point of intersection of the swelling line and the CSL in the $v-\ln p'$ space as depicted in Fig. 1.

Substituting Eq. (9) into the general stress–state relationship of Eq. (8) leads to a generalised yield surface in terms of the pre-consolidation pressure p'_0 (i.e. the state boundary surface along the elastic wall) as follows:

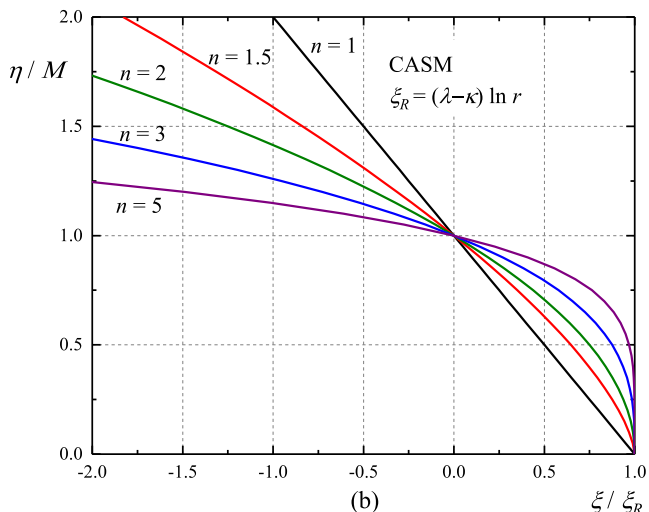
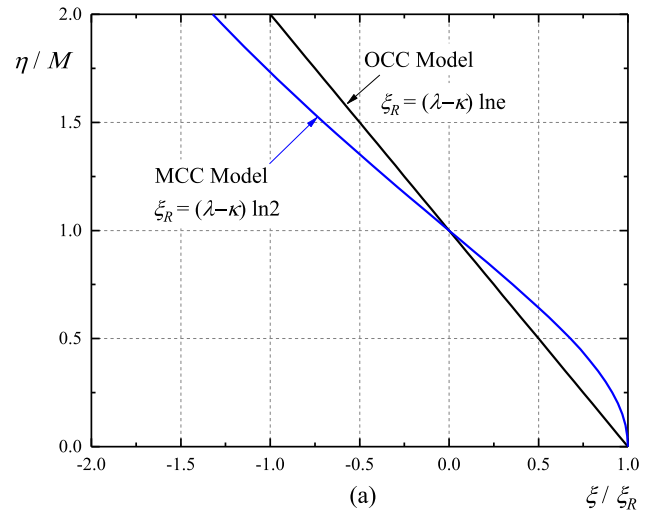


Fig. 2. Stress-state relations: (a) OCC and MCC models; and (b) CASM.

$$f = \left(\frac{q}{Mp'}\right)^n + \frac{\ln(p'/p'_0)}{\ln r} \tag{10}$$

where the preconsolidation pressure p'_0 controls the size of the yield surface as a hardening parameter, n defines the shape of the yield surface, and r controls the intersection position of the CSL and the yield surface (i.e. at $p' = p'_0/r$). As the over-consolidation ratio (OCR) is widely used to define the stress history of clay, it is useful to note that a direct relationship between the state parameter and OCR can be derived, namely, $\xi = (\lambda - \kappa)\ln(r/OCR)$.

A total of seven model constants are needed to fully define the unified critical state model CASM, five of which are the same as the standard Cam-clay models of OCC and MCC (namely, λ, κ, μ, M , and Γ). For the remaining two new material constants, n typically ranges between 1 and 5, and r typically lies in the range of 1.5–3 for clays but for sands the value of r is generally much larger (Coop and Lee, 1993; Crouch et al., 1994; Yu, 1998).

A simple procedure of determining all the model constants from triaxial tests has been presented by Yu et al. (2005). It should be noted that the OCC model can be recovered exactly from CASM by choosing $n = 1$ and $r = 2.718$. As shown in Fig. 3a, the ‘wet’ side of the MCC model can also be matched accurately by CASM by choosing $r = 2$ in conjunction with a suitable value of n (typically around 1.5–2). Fig. 3b shows that, unlike the OCC and MCC models,

the intersection point between the CSL and the yield surface in CASM does not necessarily occur at the maximum deviatoric stress. This novel feature is very important and it enables CASM to reproduce many observed yield surfaces for sand where the deviatoric stress often reaches a local peak before approaching the critical state (Sladen et al., 1985; Lade and Yamamuro, 1996; Yang, 2002; Yu et al., 2005).

Apart from soils, the critical state concept has also been applied to modelling weak porous rocks (Gerogiannopoulos and Brown, 1978; Elliott, 1983; Brown and Yu, 1988; Carroll, 1991; Baud et al., 2006; Navarro et al., 2010). In particular, Brown and Yu (1988) pointed out that the MCC model may significantly overestimate the plastic volumetric strain increments of porous rock if it is applied directly. To account for the mechanism by which frictional work can be done at sensibly constant plastic volumetric strain, a stress ratio coefficient β was therefore introduced by Brown and Yu (1988) to modify the MCC yield function for modelling porous rock (i.e. with a new yield function being defined by $q = \beta Mp'(p'_0/p' - 1)^{1/2}$). The yield function defined by CASM is compared with that proposed by Brown and Yu (1988) for describing the ductile yield of porous rock in Fig. 4. As shown in Fig. 4, the yield surfaces given by both CASM and Brown and Yu’s model can fit well with the experimental data of Elliott (1983) for Bath stone on the ductile side (i.e. the ‘wet’ side commonly known in soil mechanics) with suitable values of materials constants.

In modelling porous rock behaviour on the brittle side (or ‘dry’ side), it is often observed that the failure stress can be significantly overpredicted by the standard Cam-clay yield surfaces. To overcome this limitation, the Hvorslev surface or other empirical curves has often been introduced separately for modelling the behaviour on the brittle side (Price and Farmer, 1981; Wong et al., 1997). It is noted, however, that CASM is able to provide a much simpler alternative for defining the yield surface of porous rocks over both brittle and ductile ranges.

2.2. Hardening rule

In the unified critical state model CASM, the volumetric hardening law (i.e. Eq. (11)) is adopted as in the standard Cam-clay models. In other words, the change in the yield surface size is assumed to be a linear function of the incremental plastic volumetric strain (de_p^p) for a given stress state, namely:

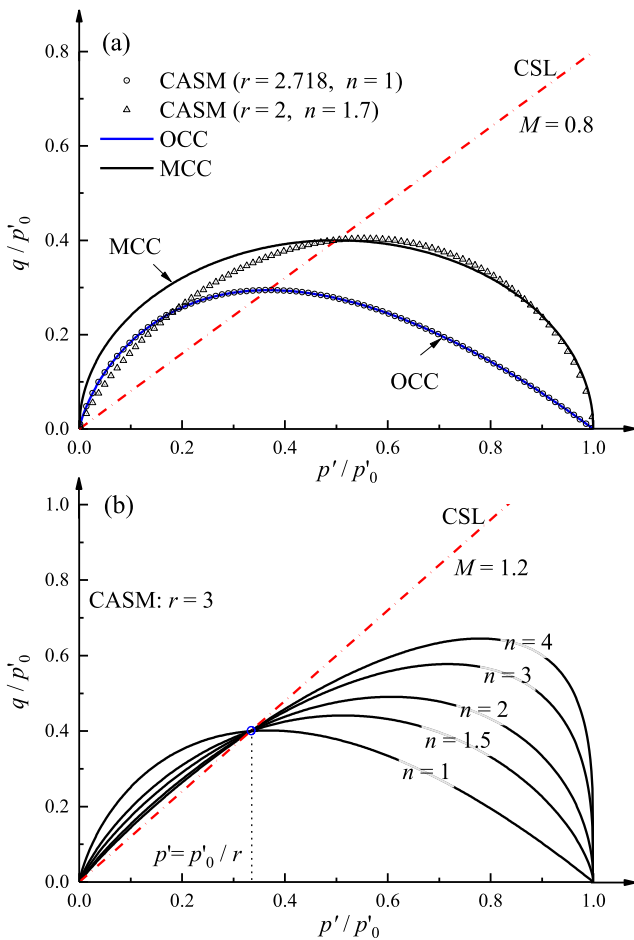


Fig. 3. (a) Comparisons of yield surfaces of OCC, MCC, and CASM; and (b) Example yield surfaces of CASM.

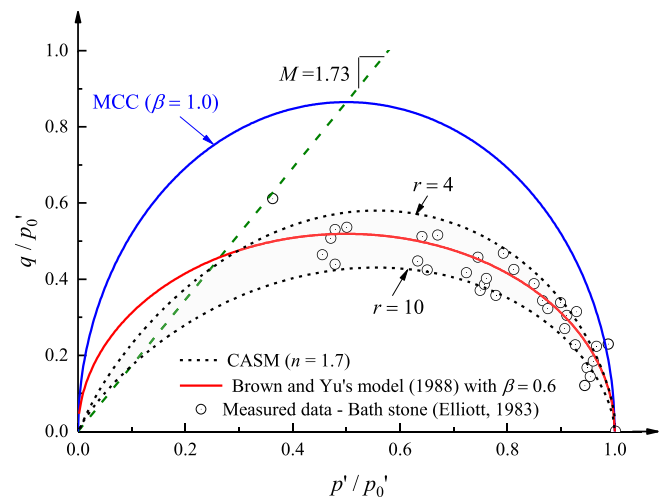


Fig. 4. Normalised yield surfaces of MCC, CASM, and the model of Brown and Yu (1988) for porous rock.

$$dp'_0 = \frac{vp'}{\lambda - \kappa} de_p^p \quad (11)$$

where e_p^p is the plastic volumetric strain.

As shown by Yu et al. (2005) and Yu (2006), it is also straightforward to extend this volumetric hardening law to a combined volumetric and deviatoric hardening law.

2.3. Stress-dilatancy relation and plastic potential

To determine plastic strains, a plastic potential is often assumed to be associated with a yield surface. The unified critical state model CASM originally adopted Rowe's stress–dilatancy relation (Rowe, 1962) as a basis to derive a plastic potential. The Rowe's plastic flow rule was originally developed from the minimum energy considerations of particle sliding and has been widely used for modelling both sands and clays. However, it has been shown that Rowe's relation may not be very realistic for stress paths with low stress ratios (e.g. one-dimensional consolidation) (Yu, 2006; Hu et al., 2018). To overcome this limitation, Yu (2006) proposed a general stress–dilatancy relation which is in a similar form to the yield function in CASM but gives zero plastic volumetric strain increment at critical states. Both of these two stress-dilatancy relations are presented as follows:

(1) Rowe's stress-dilatancy relation

$$\frac{de_p^p}{de_q^p} = \frac{9(M - \eta)}{9 + 3M - 2M\eta} \quad (12)$$

where e_q^p is the plastic deviatoric strain.

By integrating Eq. (12), the plastic potential can be shown to take the following form:

$$g_R = 3M \ln\left(\frac{p'}{C}\right) + (3 + 2M) \ln\left(\frac{2q}{p'} + 3\right) - (3 - M) \ln\left(3 - \frac{q}{p'}\right) \quad (13)$$

where C is a size parameter that can be determined easily for any stress state by setting the above equation to zero with the current stress values.

(2) A general stress-dilatancy relation by Yu (2006)

$$\frac{de_p^p}{de_q^p} = \frac{M^n - \eta^n}{m' \eta^{n-1}} \quad (14)$$

where m' is a material constant.

Eq. (14) reduces to the associated plastic flow rule of the OCC model by setting $n = 1$ and $m' = 1$, and the plastic flow rule of the MCC model can also be obtained with $n = 2$ and $m' = 2$. By setting $m' = 1$, Eq. (14) leads to the stress-dilatancy rule of McDowell (2002) for sand. By requiring that the plastic flow rule predicts zero lateral strain for the stress state corresponding to Jaky's (Jaky, 1948) K_0 condition (Ohmaki, 1982; Alonso et al., 1990; McDowell and Hau, 2003), the following expression of m' has been given by Yu (2006):

$$m' = \frac{2}{3} \frac{\lambda}{\lambda - \kappa} \frac{[M(6 - M)]^n - (3M)^n}{(6 - M)(3M)^{n-1}} \quad (15)$$

By integrating Eq. (14), it can be shown that the plastic potential takes the following form:

$$g_Y = m' \ln \left[1 + (m' - 1) \left(\frac{\eta}{M} \right)^n \right] + n(m' - 1) \ln \left(\frac{p'}{C} \right) \quad (16)$$

where C indicates the size of the plastic potential surface, which can be easily obtained by setting the above equation to zero with the current stress values.

2.4. Elastic moduli

The soil behaviour inside the yield surface is assumed to be isotropic and purely elastic in the unified critical state model CASM. The elastic stress–strain relationship is fully defined by two stress-dependent elastic moduli, namely the bulk modulus (K) and shear modulus (G) as follows:

$$K = \frac{dp}{de_p^e} = \frac{1 + e}{\kappa} p' = \frac{vp'}{\kappa} \quad (17)$$

$$G = \frac{3(1 - 2\mu)K}{2(1 + \mu)} = \frac{3(1 - 2\mu)}{2(1 + \mu)} \frac{vp'}{\kappa} \quad (18)$$

where μ is the Poisson's ratio and is assumed to be a constant, and e_p^e is the elastic volumetric strain. From a theoretical point of view, it would be preferable to assume a constant value of shear modulus, as it may be shown that the use of a constant Poisson's ratio would lead to a non-conservative model in the sense that it may not conserve energy during closed stress cycles (Zytynski et al., 1978). However, this effect may not be so important for applications to static problems. In order to better model soil behaviour under cyclic loading conditions, an extension of CASM was given by Yu et al. (2007a) using the framework of bounding surface plasticity.

2.5. Formulation for general stress states

The formulations of CASM presented so far were developed for the case of a triaxial stress condition. As shown in Yu (2006), their generalisation to a general 3D stress condition can be achieved by using the general expressions of stress variables (and corresponding strain variables) and treating M in the yield function as a variable $M(\theta_1)$ defined as

$$M(\theta_1) = M_{\max} \left[\frac{2Q^4}{1 + Q^4 + (1 - Q^4) \sin(3\theta_1)} \right]^{\frac{1}{4}} \quad (19)$$

where θ_1 is the Lode's angle; M_{\max} is the slope of the CSL under a triaxial compression (i.e. $\theta_1 = -30^\circ$) in the q - p' plane, and $Q = (3 - \sin \phi'_{cs}) / (3 + \sin \phi'_{cs})$, where ϕ'_{cs} is the critical state friction angle. With Eq. (19), the intersection of the yield surface of CASM on the deviatoric (π) plane is assumed to have a similar shape to the Matsuoka-Nakai criterion (Matsuoka and Nakai, 1974; Sheng et al., 2000).

2.6. Example prediction and validation

To assess the performance of the unified critical state model CASM in modelling stress–strain behaviour of clay and sand, an extensive experimental programme of validation has been carried out by Yu and his co-workers (Yu, 1998; Khong, 2004; Wang, 2005; Yu et al., 2005). For the purpose of illustration, example results of the application of CASM to predict measured stress–strain

behaviour of clay and sand in the laboratory under both drained and undrained loading conditions are presented in Figs. 5–12.

Taking soil material constants $\Gamma = 2.06$, $\lambda = 0.093$, $\kappa = 0.025$, $M = 0.9$, $\mu = 0.3$, $r = 2.714$, and $n = 4.5$, the predictions made by CASM are compared with test data from the classic series of triaxial compression tests performed on remoulded Weald clay by Bishop and Henkel (1957). Comparisons in Figs. 5 and 6 indicate that the predictions of CASM are consistently better than those by the OCC model for both normally and overconsolidated clays in both drained and undrained triaxial tests. In particular, CASM is found to be able to capture reasonably well the overall behaviour of the overconsolidated clay as observed in the laboratory.

The predictive performance of CASM for sand is illustrated by comparing with triaxial test results for typical quartz sands reported by Been and Jefferies (1985), Jefferies (1993), Wang (2005) and Yu et al. (2005). Fig. 7 shows a comparison of drained compression tests on loose, medium dense, and very dense Erksak 330/0.7 sand (with material constants: $\Gamma = 1.8167$, $\lambda = 0.0135$, $\kappa = 0.005$, $M = 1.2$, $\mu = 0.3$, $r = 6792$, and $n = 4$ (Yu, 1998)). Fig. 8 gives a comparison between the prediction by CASM and the data measured in both compression and extension tests on Portaway sand under undrained condition (with material constants: $\Gamma = 1.796$, $\lambda = 0.025$, $\kappa = 0.005$, $M = 1.19$, $M_e = 0.7$ (the slope of the CSL in the $q - p'$ space under extension), $\mu = 0.16$, $n = 3.5$, and $r = 19.2$ (Yu et al., 2005)). Overall, CASM can give satisfactorily accurate predictions of measured drained and undrained behaviours of sand at different initial states in both compression and extension tests. However, it has also been observed that CASM tends to underpredict the axial strains for both drained and undrained triaxial tests at peak strengths. Also, a sudden stiffness transition in the stress–strain curves is predicted by CASM for dense sands. These limitations, common to most elasto-plastic models, have been removed later in an extension of CASM using

the framework of bounding surface plasticity (i.e. allowing plastic strains to occur within the main yield surface) (Yu and Khong, 2002; Yu et al., 2005).

To illustrate the effect of the newly introduced material model constants r and n on the prediction of CASM, results calculated with different values of r and n are compared with typical drained test data on both dense (sample: CIDC-5) and loose (sample: CIDC-1) Portaway sands in Figs. 9–12 (after Wang, 2005). It is shown that their effects are opposite for a sand with a dense initial state and that with a loose initial state.

3. Cavity contraction in critical state soils

Cavity expansion/contraction analysis in soil or rock is concerned with the theoretical study of changes in stresses, displacements and pore water pressures caused by the expansion or contraction of a cylindrical or spherical cavity embedded in soil or rock. As reviewed by Yu (2000), the cavity expansion/contraction solutions can provide a simple but useful theoretical tool for modelling a range of complex geotechnical problems including in situ testing (e.g. cone penetration tests, pressuremeter tests, and dilatometer tests), pile foundations, earth anchors, underground excavation and tunnelling, and wellbore instability problems.

Over many years, a large number of cavity expansion/contraction solutions have been developed (Hoek and Brown, 1980; Yu, 2000). Significant progress has been made since the 1970s in developing analytical and semi-analytical cavity expansion solutions by using increasingly more realistic constitutive models (Vesic, 1972; Randolph and Wroth, 1979; Brown et al., 1983; Carter et al., 1986; Yu and Houlsby, 1991; Salgado et al., 1997; Sharan, 2008; Park, 2014; Chen and Abousleiman, 2017; Zhuang et al., 2018). In particular, since the pioneering work of Collins et al. (1992), Collins and Stimpson (1994), and Collins and Yu (1996),

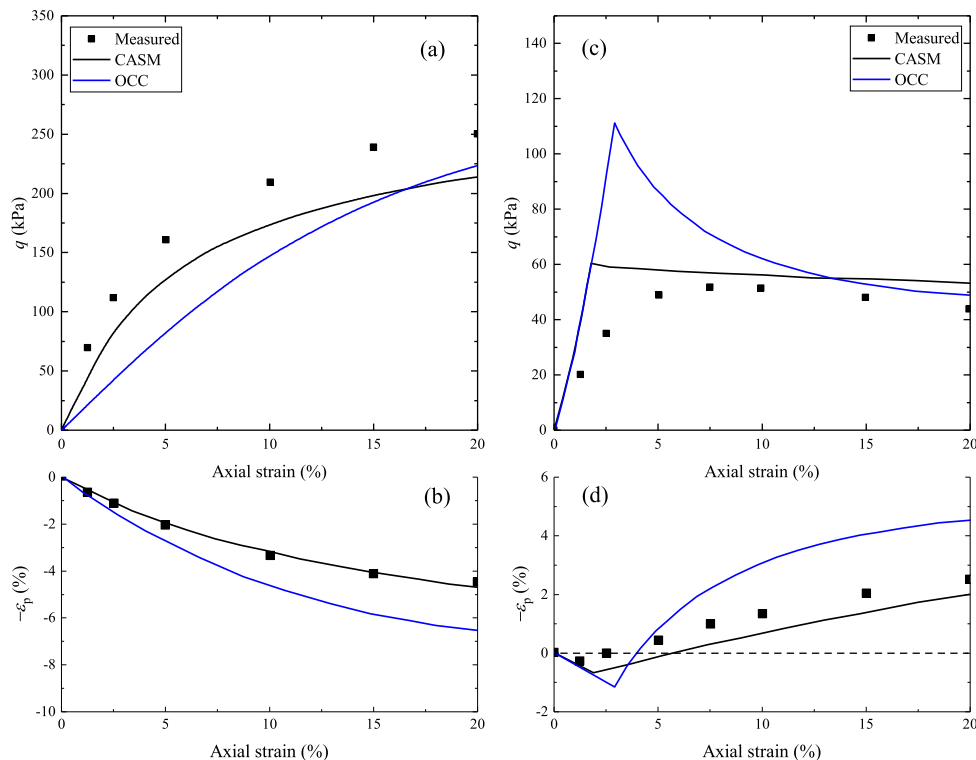


Fig. 5. Model predictions for drained compression tests on Weald clay: (a) and (b) normally consolidated sample ($OCR = 1$, $v_0 = 1.632$, and $p'_0 = 207$ kPa); and (c), (d) heavily consolidated sample ($OCR = 24$, $v_0 = 1.617$, and $p'_0 = 34.5$ kPa).

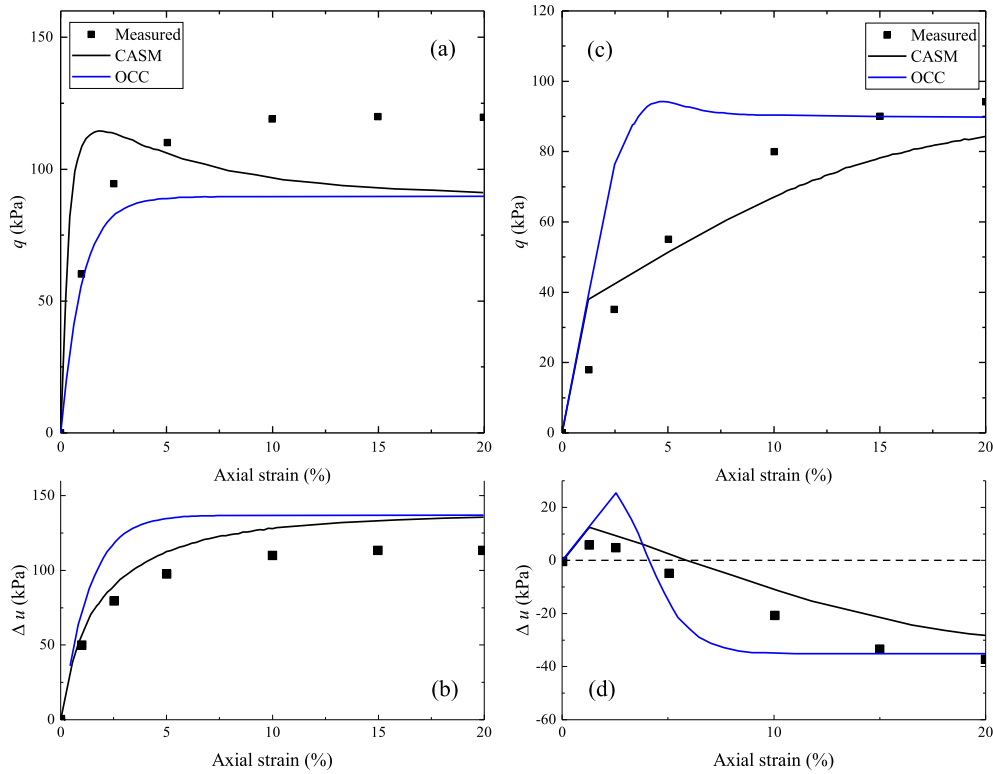


Fig. 6. Model predictions for undrained compression tests on Weald clay: (a) and (b) normally consolidated sample ($OCR = 1$, $v_0 = 1.632$, and $p'_0 = 207$ kPa); and (c), (d) heavily consolidated sample ($OCR = 24$, $v_0 = 1.617$, and $p'_0 = 34.5$ kPa).

cavity expansion/contraction solutions based on the advanced critical state soil models have gained much attention of researchers over the past two decades (Yu and Rowe, 1999; Cao et al., 2001; Salgado and Randolph, 2001; Russell and Khalili, 2002; Chen and Abousleiman, 2012, 2013, 2016; Li et al., 2016; Vrakas, 2016b; Chen and Liu, 2018; Zhou et al., 2018). Most recently, analytical/semi-analytical solutions using the unified critical state model CASM have been derived by Mo and Yu (2017a,b, 2018) for both undrained and drained analyses of cavity expansion and undrained analysis of cavity contraction in both clay and sand.

To demonstrate the application of CASM in solving geotechnical boundary value problems, both drained and undrained cavity contraction solutions are presented in this section. They will be applied in the next section to estimating the ground response curves and ground settlements of circular tunnels in clay and sand. Whilst the undrained contraction solution follows that of Mo and Yu (2017a), new drained contraction solutions are derived in this section by following the solution procedure of Mo and Yu (2018).

3.1. Problem definition

Cavity contraction solutions have been used for decades for the prediction of ground settlements due to tunnelling and the design of tunnel support systems to maintain its stability (Hoek and Brown, 1980; Brady and Brown, 1993; Carranza-Torres and Fairhurst, 2000; Yu, 2000). Following Mair and Taylor (1993) and Yu and Rowe (1999), the behaviour of soil around a cylindrical tunnel (e.g. Fig. 13) is idealised either in terms of the unloading of a spherical cavity (around the tunnel face) or the unloading of a cylindrical cavity. If the tunnel is sufficiently deep in the ground, the ground surface effect would be small and may therefore be neglected for simplicity in the analysis. The initial ground stresses around the tunnel are simplified as hydrostatic. The tunnel

excavation is simulated by slowly reducing the internal cavity pressure from an in situ stress value (σ'_0) to a uniform pressure acting on the lining (for lined tunnels) or to zero (for unlined tunnels). Compressive stresses and strains are considered as positive here. The soil is assumed to be isotropic and its stress–strain behaviour is characterised by the unified critical state model CASM. For convenience, cylindrical coordinates (\bar{r} , θ , z) and spherical coordinates (\bar{r} , θ , φ) with the origin located at the centre of the cavity are employed to describe the spatial locations of material points in the contraction process of a cylindrical and spherical cavity, respectively. The cylindrical cavity expansion analysis is conducted under a plane strain condition along the z -axis.

Following Collins and Yu (1996), the mean and deviatoric effective stresses (p' , q) for the symmetric cavity expansion/contraction problem are expressed as

$$\left. \begin{aligned} p' &= \frac{\sigma'_{\bar{r}} + m\sigma'_{\theta}}{1 + m} \\ q &= \sigma'_{\bar{r}} - \sigma'_{\theta} \end{aligned} \right\} \quad (20)$$

where $\sigma'_{\bar{r}}$ and σ'_{θ} are the radial and circumferential effective stresses, respectively; and $m = 1$ for a cylindrical cavity and $m = 2$ for a spherical cavity.

The corresponding volumetric and shear strains (ϵ_p , γ) can be written as

$$\left. \begin{aligned} \epsilon_p &= \epsilon_{\bar{r}} + m\epsilon_{\theta} \\ \gamma &= \epsilon_{\bar{r}} - \epsilon_{\theta} \end{aligned} \right\} \quad (21)$$

where $\epsilon_{\bar{r}}$ and ϵ_{θ} are the radial and circumferential strains, respectively.

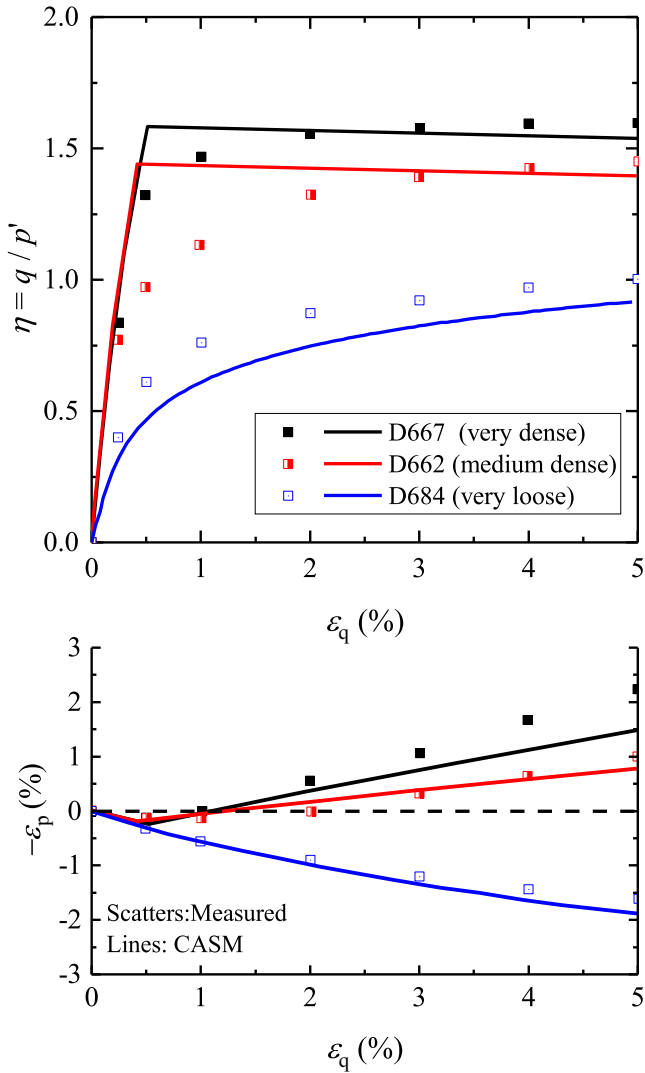


Fig. 7. Model predictions for drained compression tests on Erksak 330/0.7 sand (sample D667: $v_0 = 1.59$, $p'_0 = 130$ kPa; sample D662: $v_0 = 1.677$, $p'_0 = 60$ kPa; sample D684: $v_0 = 1.82$, $p'_0 = 200$ kPa).

The stress equilibrium condition in the radial direction during a symmetrical expansion/contraction is readily expressed as

$$\sigma_{\tilde{r}} - \sigma_{\theta} + \frac{\tilde{r}}{m} \frac{d\sigma_{\tilde{r}}}{d\tilde{r}} = 0 \quad (22)$$

where $\sigma_{\tilde{r}}$ and σ_{θ} are the radial and circumferential total stresses, respectively.

3.2. Cavity contraction under drained condition

For the fully drained cases, the analysis is conducted in terms of effective stresses with drained soil strength and deformation parameters.

(1) Elastic analysis

To be consistent with Eqs. (20) and (21), the shear modulus in the hypoelastic relationship adopted in CASM (i.e. Eqs. (17) and (18)) is applied for the cavity contraction problem as

$$G = \frac{\varpi v p'}{\kappa} \quad (23)$$

$$\text{where } \varpi = \frac{(1+m)(1-2\mu)}{2[1+(m-1)\mu]}$$

For simplicity, the small strain assumption is adopted in the purely elastic stage of analysis. It has been shown by Chen and Abousleiman (2013) and Mo and Yu (2018), the elastic stresses and the radial displacement (u_r) can be readily derived as follows:

$$\sigma_{\tilde{r}} = \sigma'_0 + (\sigma_{\tilde{r}}^{\text{in}} - \sigma'_0) \left(\frac{a}{\tilde{r}}\right)^{1+m} \quad (24)$$

$$\sigma_{\theta} = \sigma'_0 - \frac{1}{m} (\sigma_{\tilde{r}}^{\text{in}} - \sigma'_0) \left(\frac{a}{\tilde{r}}\right)^{1+m} \quad (25)$$

$$u_r = \tilde{r} - \tilde{r}_0 = \frac{\sigma_{\tilde{r}}^{\text{in}} - \sigma'_0}{2mG} \left(\frac{a}{\tilde{r}}\right)^{1+m} \tilde{r} \quad (26)$$

where $\sigma_{\tilde{r}}^{\text{in}}$ denotes the internal pressure on the cavity wall. \tilde{r} and \tilde{r}_0 represent the current and initial radius in the coordinate systems, respectively; a represents the current cavity radius.

(2) Elasto-plastic analysis

Upon continuous unloading, yielding would take place from the inner cavity wall. According to the yield criterion of CASM (i.e. Eq. (10) as illustrated in Fig. 14), the initial yielding conditions are $p' = \sigma'_0$ and $q = q_{\text{ep}}^c \cdot q_{\text{ep}}^c$ is written as

$$\left. \begin{aligned} q_{\text{ep}}^c &= - \left(\frac{\ln R_0}{\ln r} \right)^{\frac{1}{n}} M_e \sigma'_0 \\ R_0 &= p'_{0,0} / \sigma'_0 \end{aligned} \right\} \quad (27)$$

where $p'_{0,0}$ is the initial yield pressure under an isotropic consolidation.

The elasto-plastic boundary will propagate inside the surrounding soil with further unloading. The incremental form of the stress–strain relationship in the elastic region can be expressed as follows:

$$D\varepsilon_p^e = -\frac{Dv}{v} = \frac{Dp'}{K} \quad (28)$$

$$D\gamma^e = \frac{1}{2G} Dq \quad (29)$$

where D denotes the material derivative.

By using the logarithmic strains (i.e. Eq. (30)), a large strain analysis is performed in the inner plastic region:

$$\left. \begin{aligned} \varepsilon_{\tilde{r}} &= -\ln\left(\frac{d\tilde{r}}{d\tilde{r}_0}\right) \\ \varepsilon_{\theta} &= -\ln\left(\frac{\tilde{r}}{\tilde{r}_0}\right) \end{aligned} \right\} \quad (30)$$

Following Chen and Abousleiman (2013) and Mo and Yu (2018), the auxiliary variable χ ($\chi = u_r/\tilde{r} = (\tilde{r} - \tilde{r}_0)/\tilde{r}$) is introduced. The strains can then be expressed in terms of χ as follows:

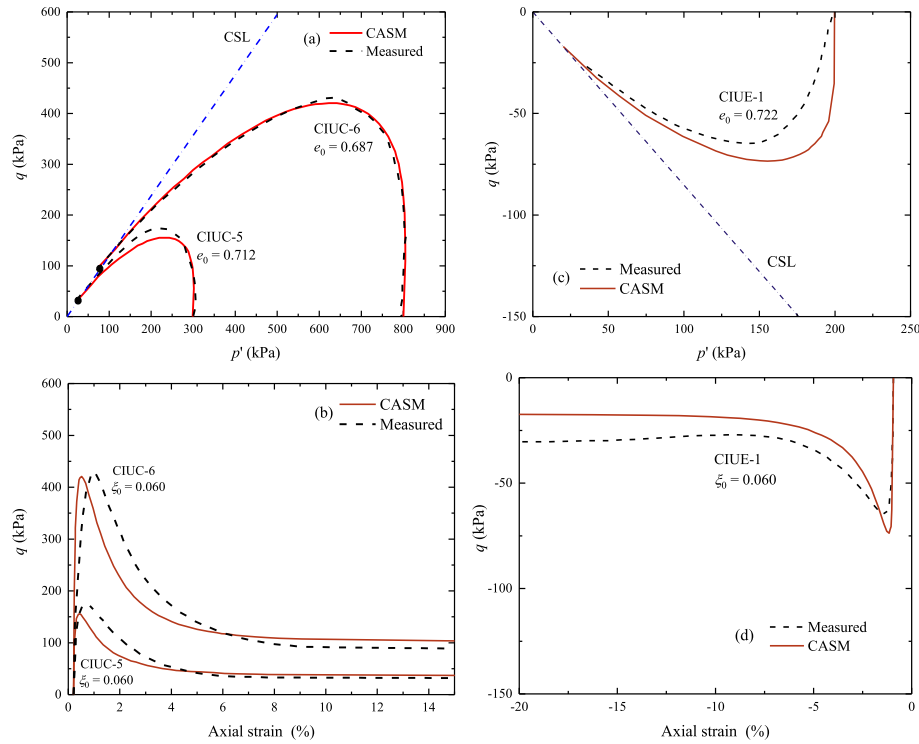


Fig. 8. Model predictions of undrained tests on very loose Portaway sand: (a) and (b) compression tests; and (c) and (d) extension tests.

$$\varepsilon_\theta = -\ln\left(\frac{\tilde{r}}{\tilde{r}_0}\right) = \ln(1 - \chi) \quad (31)$$

$$\varepsilon_{\tilde{r}} = \varepsilon_p - m\varepsilon_\theta = -\ln\left[\frac{v}{v_0}(1 - \chi)^m\right] \quad (32)$$

$$\gamma = \varepsilon_{\tilde{r}} - \varepsilon_\theta = -\ln\left[\frac{v}{v_0}(1 - \chi)^{m+1}\right] \quad (33)$$

In the fully drained analysis, the excess pore pressure equals zero during a continuous cavity contraction. With the aid of χ , the equilibrium requirement for the cavity contraction problem (i.e. Eq. (22)) can be converted into the Lagrangian form as

$$q + \frac{Dp' + \frac{m}{m+1}Dq}{mD\chi} \left[1 - \chi - \frac{v_0}{v(1 - \chi)^m}\right] = 0 \quad (34)$$

The incremental volume and deviatoric strains within the plastic region are given by

$$D\varepsilon_p = -\frac{Dv}{v} = D\varepsilon_p^e + D\varepsilon_p^p = \kappa \frac{Dp'}{vp'} + \frac{\lambda - \kappa}{v} \frac{Dp'_0}{p'_0} \quad (35)$$

$$\begin{aligned} D\gamma &= -\frac{Dv}{v} + \frac{m+1}{1-\chi}D\chi = D\gamma^e + D\gamma^p \\ &= \frac{\kappa Dq}{2\sigma vp'} - \frac{\lambda - \kappa}{v} \frac{Dp'_0}{p'_0} \frac{m+1}{m} \frac{9+3M-2M\eta}{9(M-\eta)} \end{aligned} \quad (36)$$

where it should be noted that $\eta = -q/p'$ under unloading. Now the stress–strain analysis in the plastic region is turned into a problem of solving Eqs. 34–36 to compute Dv , Dq , and Dp' (or $D\chi$) with a given $D\chi$ (or Dp') from the elasto-plastic boundary to the inner cavity wall. The equivalent position of a material particle

around the cavity at \tilde{r} corresponding to the auxiliary variable χ is revived by integration from a to \tilde{r} as follows:

$$\int_a^{\tilde{r}} \frac{d\tilde{r}}{\tilde{r}} = \ln \frac{\tilde{r}}{a} = \int_{\chi|\tilde{r}=a}^{\chi} \frac{d\chi}{1 - \chi - v_0/[v(1 - \chi)^m]} \quad (37)$$

From Eq. (37), the radius of the elasto-plastic boundary (\tilde{r}_c) can be obtained. Then the stresses and displacement within the outer elastic region can be calculated from Eqs. (24)–(26) by replacing a and $\sigma_{\tilde{r}}^{\text{in}}$ with \tilde{r}_c and $\sigma'_0 - q_{ep}^c/(1 + m)$, respectively.

3.3. Cavity contraction under undrained condition

For a cavity unloading from the initial cavity pressure of σ'_0 , the initial contraction is purely elastic (Yu and Rowe, 1999). After an initial yielding at the cavity wall, three regions (i.e. elastic, plastic, and critical-state regions) would be formed around the inner cavity during a continuous contraction in the undrained analysis. \tilde{r}_c and \tilde{r}_{cs} are used to represent the interface radius between the elastic region and the plastic region, and that between the plastic region and the critical-state region, respectively. The elasto-plastic solutions of Mo and Yu (2017a) are summarised as follows.

Given the undrained condition, the soil volume within an arbitrary radius (\tilde{r}) can be assumed to be constant, and this condition can be expressed as

$$\tilde{r}_0^{m+1} - \tilde{r}^{m+1} = a^{m+1} - a^{m+1} = T \quad (38)$$

The constant-volume condition of Eq. (38) is very useful in both elastic and elasto-plastic analyses, which simplifies the solution process of cavity contraction problems. By solving Eq. (38) along with the equilibrium equation of Eq. (22), and the stress–strain equations in CASM, the following analytical solutions can be obtained.

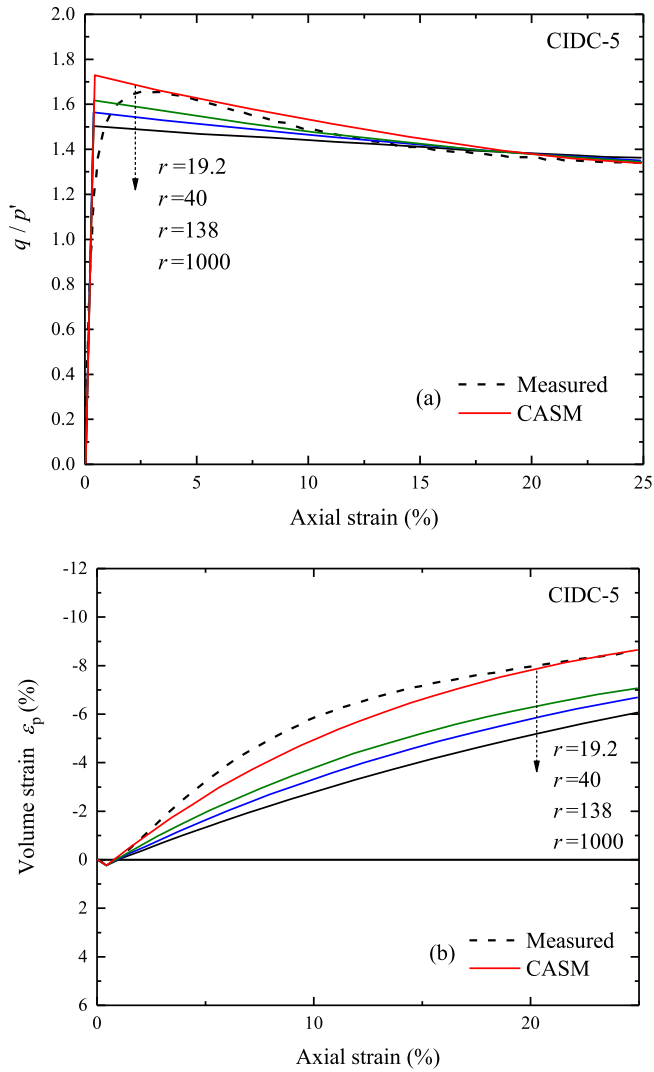


Fig. 9. Effect of the spacing ratio r on predicted behaviour of dense Portaway sand.

(1) Solution for the elastic region

The effective stresses ($\sigma'_r, \sigma'_\theta$), total stresses (σ_r, σ_θ) and strains ($\epsilon_r, \epsilon_\theta$) in the elastic region ($\tilde{r}_c < \tilde{r}$) can be expressed by Eqs. (39)–(41), respectively:

$$\left. \begin{aligned} \sigma'_r &= \sigma'_0 - mA(\tilde{r}) \\ \sigma'_\theta &= \sigma'_0 + A(\tilde{r}) \end{aligned} \right\} \quad (39)$$

$$\left. \begin{aligned} \sigma_r &= \sigma'_0 + 2G_0mB(\tilde{r}) \\ \sigma_\theta &= \sigma'_0 + 2G_0mB(\tilde{r}) + (m + 1)A(\tilde{r}) \end{aligned} \right\} \quad (40)$$

$$\left. \begin{aligned} \epsilon_r &= \frac{-m}{2G_0}A(\tilde{r}) \\ \epsilon_\theta &= \frac{1}{2G_0}A(\tilde{r}) \end{aligned} \right\} \quad (41)$$

where

$$A(\tilde{r}) = \frac{2G_0}{m + 1} \ln \left(\frac{\tilde{r}^{m+1} + T}{\tilde{r}^{m+1}} \right)$$

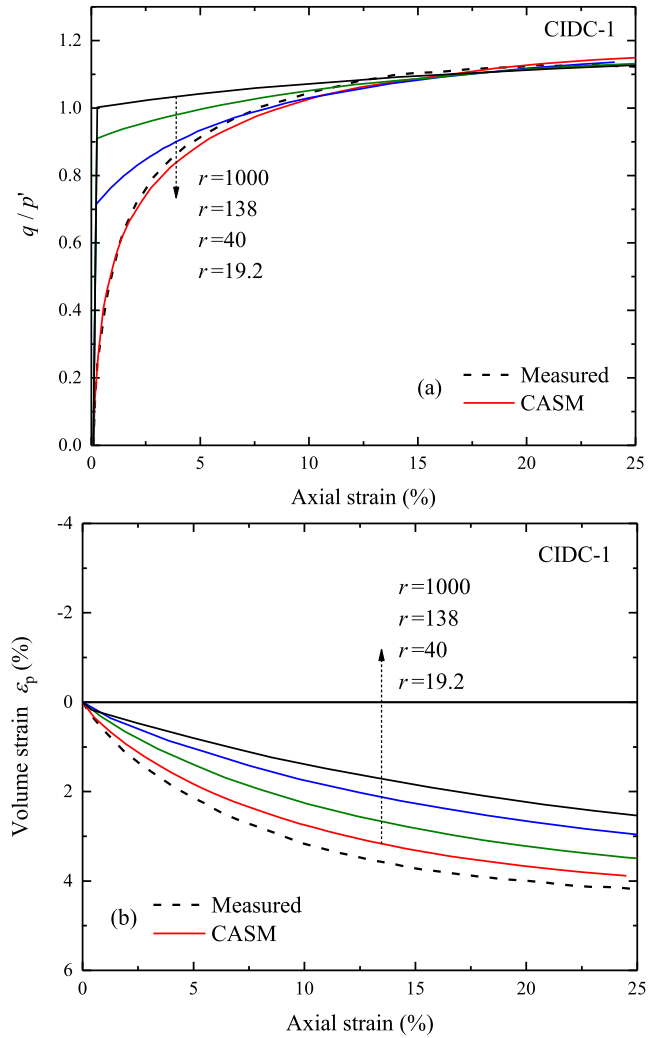


Fig. 10. Effect of the spacing ratio r on predicted behaviour of very loose Portaway sand.

$$B(\tilde{r}) = \frac{1}{m + 1} \sum_{k=1}^{\infty} \frac{(-T/\tilde{r}^{m+1})^k}{k^2}$$

$$G_0 = G(\sigma'_0)$$

Based on the yield criterion of Eq. (10) and the above elastic stress components, the current radius of the elasto-plastic boundary and its original position before cavity contraction occurs can be explicitly obtained as follows:

$$\left. \begin{aligned} \tilde{r}_c &= \left\{ -T / \left\{ 1 - \exp \left[\left(\frac{\ln R_0}{\ln r} \right)^{\frac{1}{2}} \frac{M_e \sigma'_0}{2G_0} \right] \right\} \right\}^{\frac{1}{m+1}} \\ \tilde{r}_{c0} &= (\tilde{r}_c^{m+1} - T)^{\frac{1}{m+1}} \end{aligned} \right\} \quad (42)$$

(2) Solution for the plastic region

Based on CASM and the constant-volume condition of Eq. (38), the elastic volumetric strain, plastic volumetric strain, and elastic deviatoric strain in the plastic region ($\bar{r}_{cs} < \bar{r} < \bar{r}_c$) are given as follows:

$$\left. \begin{aligned} \epsilon_p^e &= \frac{\kappa}{\nu} \ln\left(\frac{p'}{\sigma'_0}\right) \\ \epsilon_p^p &= \frac{\lambda - \kappa}{\nu} \ln\left(\frac{p'_0}{p'_{0,0}}\right) \end{aligned} \right\} \quad (43)$$

$$\epsilon_q^e = \frac{-(m+1)}{2G_0} A(\bar{r}_c) - \frac{[1 + (m-1)\mu]\kappa M}{(m+1)(1-2\mu)\nu} \left[\frac{n}{(1+n)A_2} (A_1 + A_2 \ln p')^{\frac{1}{n}+1} (A_1 + A_2 \ln p)^{\frac{1}{n}} - \frac{n}{(1+n)A_2} (A_1 + A_2 \ln \sigma'_0)^{\frac{1}{n}+1} - (A_1 + A_2 \ln \sigma'_0)^{\frac{1}{n}} \right] \quad (44)$$

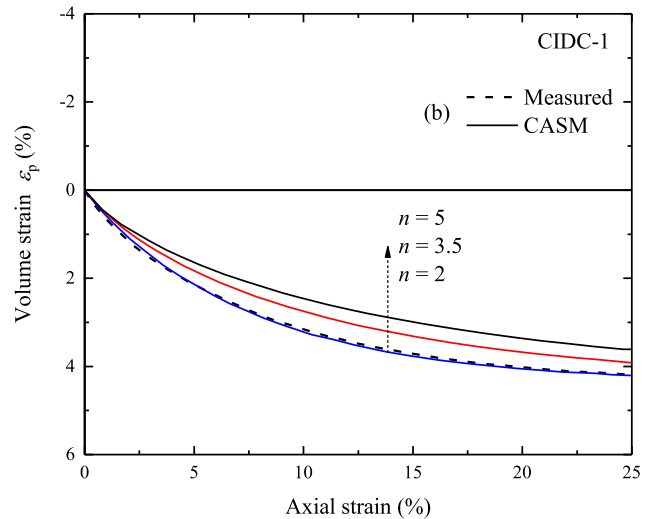
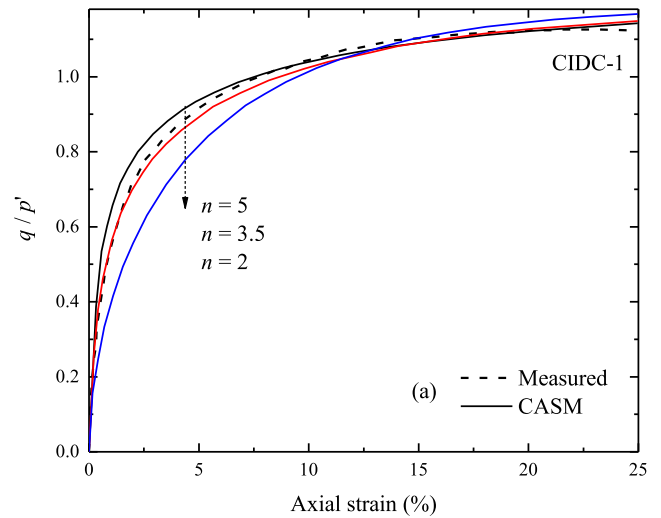
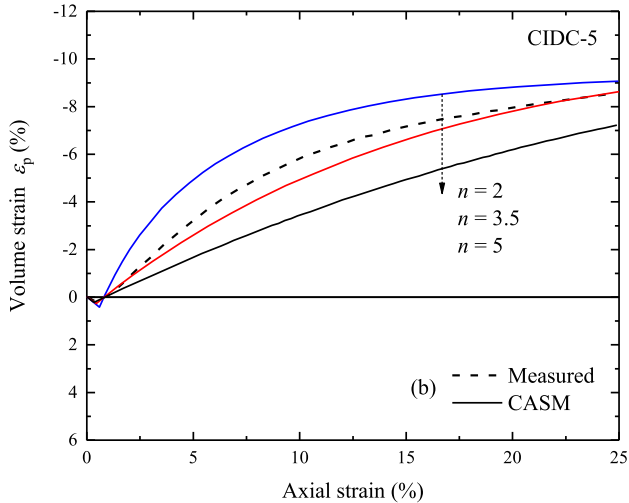
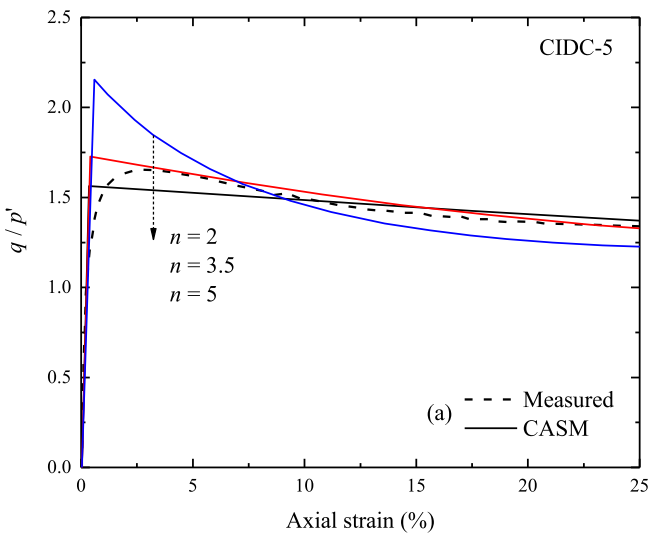


Fig. 11. Effect of the stress–state coefficient n on predicted behaviour of dense Portaway sand.

Fig. 12. Effect of the stress–state coefficient n on predicted behaviour of loose Portaway sand.

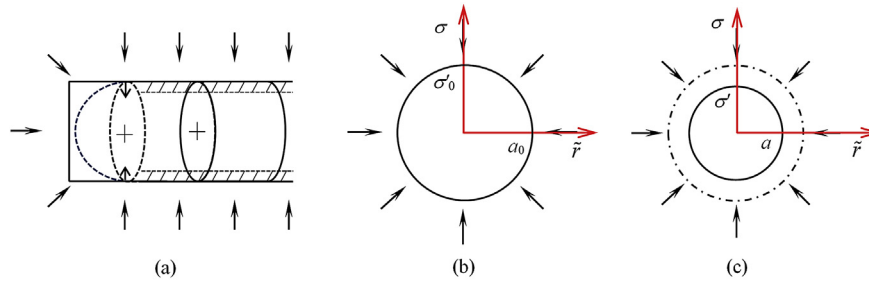


Fig. 13. Geometry of a tunnel and cavity: (a) idealisation of a circular tunnel; (b) an initial cavity; and (c) a contracted cavity.

where

$$A_1 = \frac{\ln R_0 + A^{-1} \ln \sigma'_0}{\ln r}$$

$$A_2 = -\frac{A^{-1}}{\ln r}$$

$$A = \frac{\lambda - \kappa}{\lambda}$$

Using Rowe's flow rule for unloading, namely $de_p^p/de_q^p = -9(M_e - \eta)/(9 + 3M_e - 2M_e\eta)$, the plastic deviatoric strain is obtained as follows:

$$\epsilon_q^p = \frac{\kappa n(m+1)}{9\nu A_2 M_e^n m} \left[\frac{2M_e}{n} (\eta^n - \eta_c^n) + (9 + 3M_e - 2M_e^2) \cdot \int_{\eta_c}^{\eta} \frac{\eta^{n-1}}{M_e - \eta} d\eta \right] \quad (45)$$

where

$$\eta_c = -q_{ep}^c / \sigma'_0$$

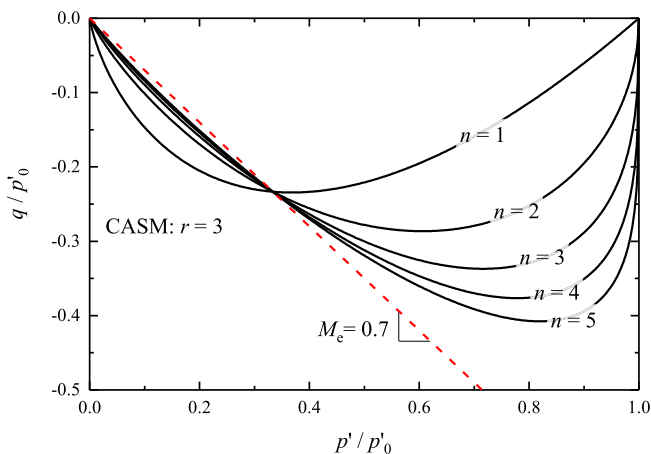


Fig. 14. Example yield surfaces of CASM under extension.

$$\int \frac{\eta^{n-1}}{M_e - \eta} d\eta = \begin{cases} 0 & (\eta_c = M_e) \\ \frac{\eta^n}{M_e} \sum_{k=0}^{\infty} \left[\frac{1}{n+k} \left(\frac{\eta}{M_e} \right)^k \right] & (\eta_c < M_e) \\ \sum_{k=0}^{\infty} \left[-M_e^k \frac{\eta^{n-1-k}}{n-1-k} \right] & (\eta_c > M_e) \end{cases} \quad (46)$$

According to the quasi-static equilibrium equation of Eq. (38), the total stresses and the excess pore pressure can be calculated by numerical integration of Eq. (47):

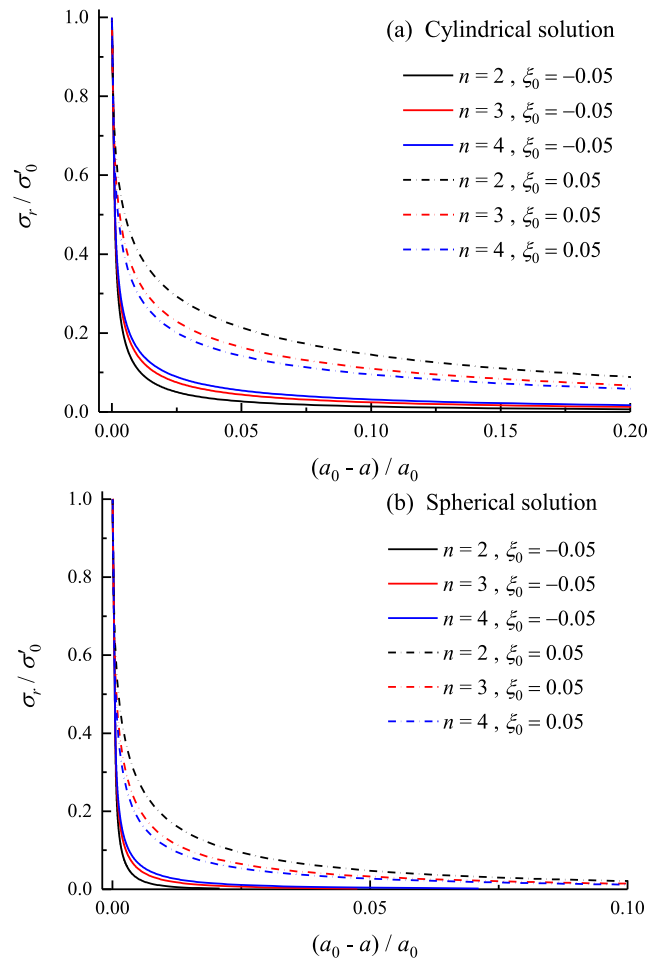


Fig. 15. Normalised cavity contraction curves with different values of the stress-state coefficient n ($\sigma'_0 = 200$ kPa): (a) cylindrical solution; and (b) spherical solution.

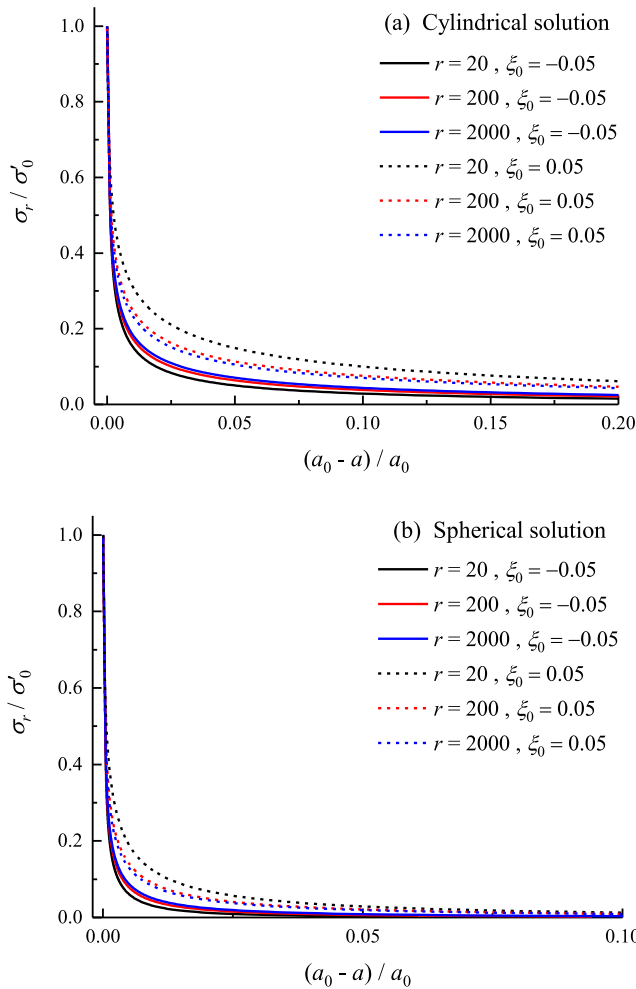


Fig. 16. Normalised cavity contraction curves with different values of the spacing ratio r ($\sigma'_0 = 200$ kPa): (a) cylindrical solution; and (b) spherical solution.

$$\int d\sigma_{\tilde{r}} = -m \int \frac{q}{\tilde{r}} d\tilde{r} \quad (47)$$

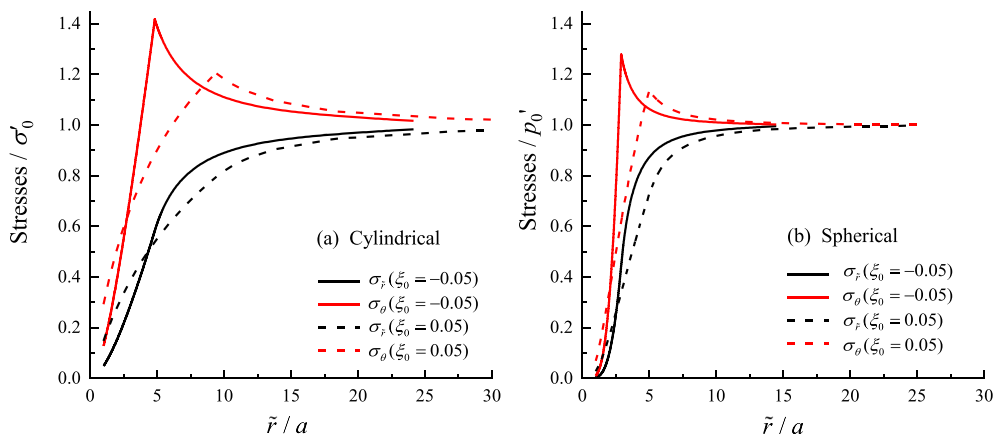


Fig. 17. Stress distribution with cavity contraction of $(a_0 - a)/a_0 = 5\%$ ($\sigma'_0 = 200$ kPa): (a) cylindrical solution; and (b) spherical solution.

(3) Solution for the critical-state region

With further unloading after the plastic deformation stage, soil in the plastic zone may reach the critical-state starting from the inner cavity wall. In the critical-state zone ($a < \tilde{r} < \tilde{r}_{cs}$), the deviatoric and mean effective stresses remain constant and are given below:

$$\left. \begin{aligned} p'_{cs} &= \left(\frac{R_0}{r}\right)^{\lambda} \sigma'_0 = \exp\left(\frac{\Gamma - v}{\lambda}\right) \\ q_{cs} &= -M_e p'_{cs} \\ p'_{0,cs} &= p'_{cs} r \end{aligned} \right\} \quad (48)$$

4. Prediction of ground response curves and settlements of tunnels

The interaction of stresses and displacements in the soil surrounding a tunnel and in the lining or support elements is commonly represented by a ground response curve (or a ground reaction curve) and a support reaction line on a ground–support interaction diagram (Brady and Brown, 1993; Carranza-Torres and Fairhurst, 2000). It is shown that cavity contraction solutions can provide a simple and useful theoretical method for estimating ground response curves (Brown et al., 1983; Mair and Taylor, 1993; Yu and Rowe, 1999; Vrakas, 2016a; Mo and Yu, 2017a). The usefulness of the cavity contraction solutions developed in the previous section in predicting the ground response curves and convergence (inward displacements) of the soil surrounding a tunnel during its excavation is illustrated briefly as follows.

4.1. Drained analysis

A drained cavity contraction analysis would be more suitable for estimating the ground response around a tunnel during its excavation in sand and weak rocks (Yu and Rowe, 1999; Chen and Abousleiman, 2016; Vrakas et al., 2017; Franza et al., 2018). Taking the soil constants measured for Portaway sand as given in a previous section, example cavity contraction curves are calculated, and effects of the two new material constants in CASM (i.e. r and n) are illustrated in Figs. 15 and 16. It is shown that much steeper cavity contraction curves (i.e. ground response curves) are predicted by the spherical cavity solution than the cylindrical cavity

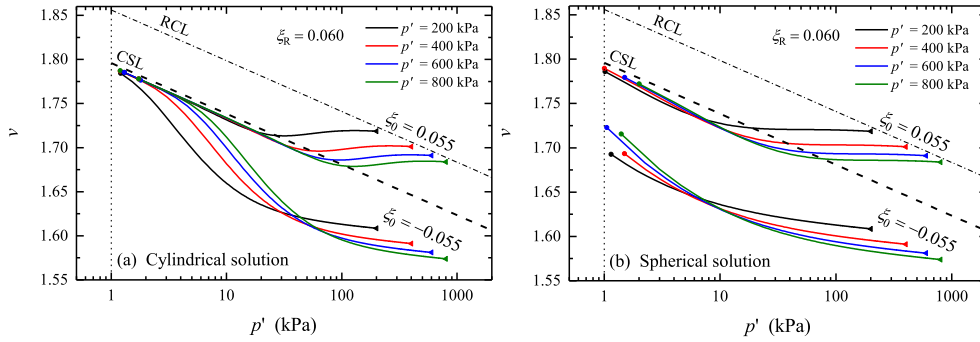


Fig. 18. Stress paths in the $v - \ln p'$ space: (a) cylindrical solution; and (b) spherical solution.

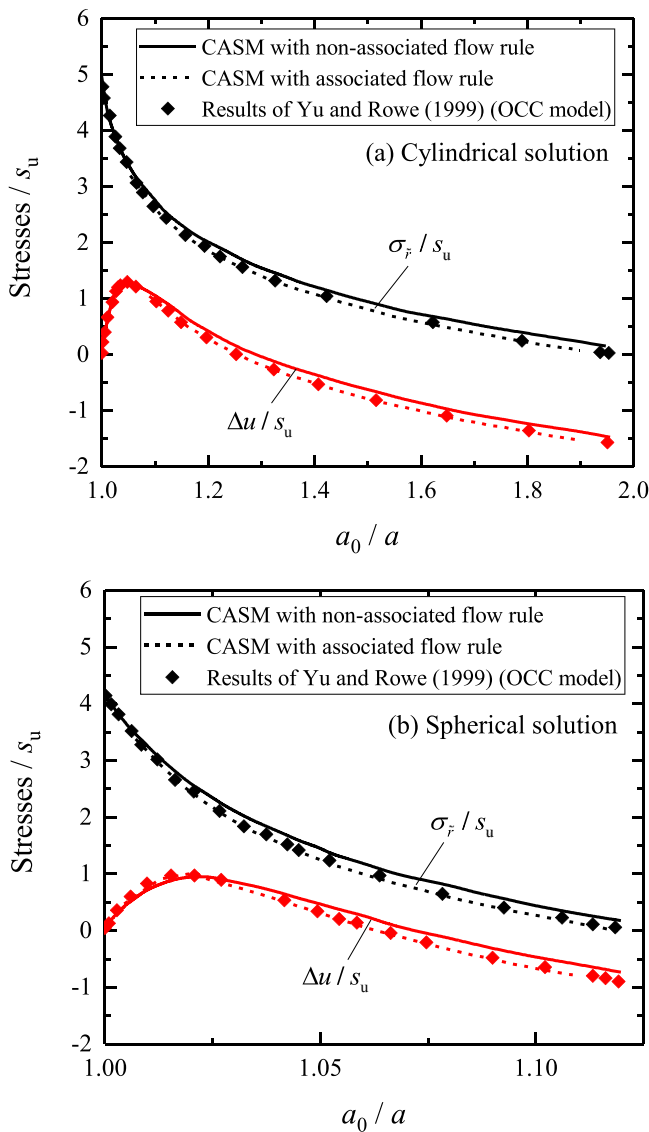


Fig. 19. Total stress and pore water pressure comparison ($R_0 = 1.001$, CASM: $n = 1$ and $r = 2.718$): (a) cylindrical solutions; and (b) spherical solutions.

solution for the same material and boundary conditions. The predicted cavity wall pressure reduces more quickly for sand with a dense initial state ($\xi_0 < 0$) than that with a loose initial state ($\xi_0 > 0$), and this is consistent with the experimental observations

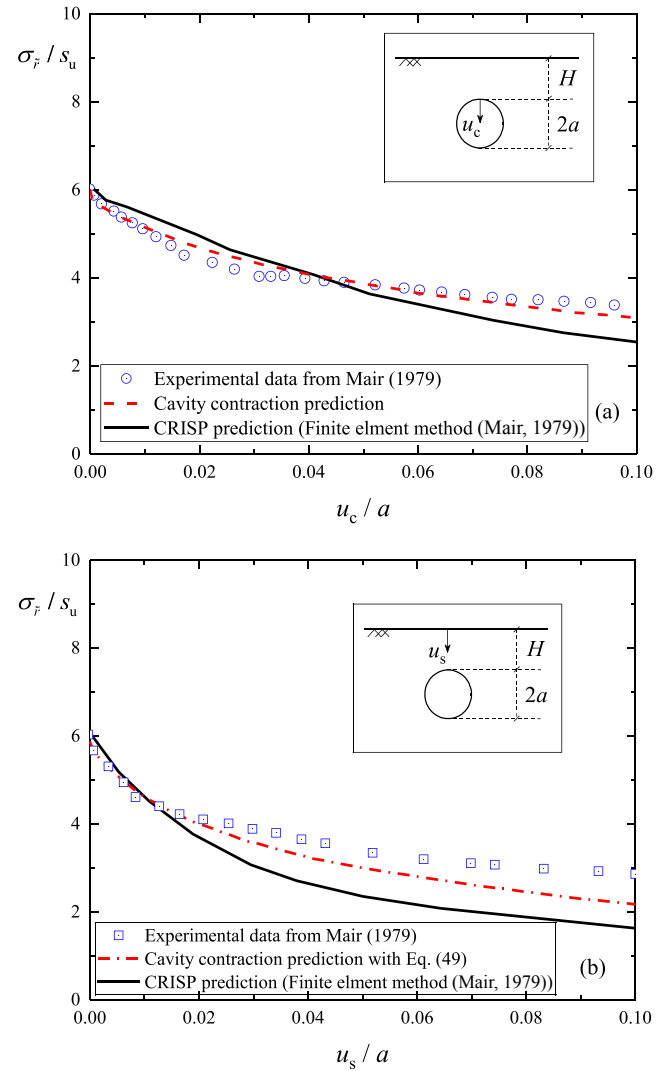


Fig. 20. Predicted and observed settlements around a tunnel in clay (Test 2DP reported in Mair (1979) with a cover to diameter ratio of 1.67): (a) tunnel crown settlements as tunnel pressure is reduced; and (b) mid-surface settlements as tunnel pressure is reduced.

of Zhou (2015) and Franza (2017) based on centrifuge tunnel tests in drained sand. As the parameters r and n control the shape of the yield surface, they would have significant effects on the predicted cavity contraction curves. Their influences are shown in Figs. 15 and

16, which are opposite for a sand with a dense initial state and that with a loose initial state.

Fig. 17 shows the differences in stress distributions around a cylindrical and a spherical cavity for the case when the level of contraction is $(a_0 - a)/a_0 = 5\%$. At the same level of contraction, the plastic zone developed around a cylindrical cavity is found to be larger than that around a spherical cavity. It is also shown to be larger in sand with a loose initial state than that in a dense state.

Stress paths during cavity contraction (i.e. unloading) in the $v - \ln p'$ space are shown in Fig. 18 for sands with two initial stress states (loose and dense states) but with four different initial mean effective stresses. For a cylindrical or spherical cavity surrounded by loose sand, the sand becomes denser during the initial stage of cavity unloading. After the sand passes through the CSL from the 'wet' side (or loose) to the 'dry' (or dense) side, its specific volume starts to increase with further unloading, and the mean effective stress decreases along a path very close to the CSL. For the sand with an initial state on the 'dry' (or dense) side, its specific volume increases monotonically whereas the distance of its current state to the CSL tends to increase initially (i.e. the sand becomes denser), after which the sand becomes looser. For a cylindrical cavity, the stress path of a dense sand moves towards the CSL. In the end, the stress ratio η is reaching towards its critical state value of M_e .

For a spherical cavity unloading, it is noted that, while the stress path of a sand with an initial state on the dry (or dense) side also moves towards the CSL, its end state may still be far away from the CSL line as η is much greater than M_e (see Fig. 18b).

4.2. Undrained analysis

Tunnel construction in clay is usually sufficiently rapid that the clay behaviour around the tunnel may be reasonably assumed to be of an undrained nature (Mair and Taylor, 1993). Ground response curves calculated by the above undrained cavity contraction solution are compared with those published by Yu and Rowe (1999) in Fig. 19 for the purpose of validation. The critical-state parameters of lightly overconsolidated (e.g. $R_0 = 1.001$) London clay are used (Yu and Rowe, 1999) as an example for comparison.

By setting $n = 1$ and $r = 2.718$ in CASM, slightly slower cavity convergence curves are predicted by the present cavity contraction solution than those predicted by the solution of Yu and Rowe (1999) (using the OCC model) due to the different flow rules used in these two solutions. However, if the Rowe's flow rule used in the present model is replaced by the associated flow rule adopted in the OCC model (e.g. $de_p^p/de_q^p = -(M_e - \eta)$), then the present solution gives the same cavity convergence curves as those of Yu and Rowe (1999), as shown Fig. 19.

The results predicted by the present cylindrical cavity contraction solution are also compared with the experimental data measured by Mair (1979) from a centrifuge tunnel test (2DP) in slightly overconsolidated Kaolin clay in Fig. 20 (assuming the soil properties as: $\Gamma = 3.92$, $\lambda = 0.3$, $\kappa = 0.05$, $M_e = 0.8$, $\mu = 0.3$, and $s_u = 26$ kPa ($s_u = 0.5M_e \exp[(\Gamma - v)/\lambda]$). From the comparison results in Fig. 20a, it can be concluded that the present cavity unloading solutions can be used to accurately predict crown settlements (u_c) around the tunnel during excavations. In contrast, these solutions tend to underpredict the observed mid-surface settlement (u_s), probably due to the effect caused by the proximity of shallow tunnels to the free ground surface.

In order to account for the free ground surface effect, it has been shown by Yu (2000) that the vertical displacement on the ground surface can be correlated with the cavity wall movement

in a simple manner as Eq. (49) by combining with the elastic unloading solution of a cavity in a half-space from Verruijt and Booker (1996). Applying Eq. (49) to the centrifuge test 2DP reported by Mair (1979), we obtain $u_s = 0.46u_c$. While the surface settlement caused by tunnelling is still slightly underestimated, Fig. 20b shows that a closer estimate can be achieved when the cavity contraction solution is used in combination with Eq. (49):

$$\frac{u_{z=0}}{u_c} = \frac{2h/B}{[(x/B)^2 + (h/B)^2]} \quad (49)$$

where $u_{z=0}$ represents the ground surface settlement due to tunnel convergence; x is the horizontal distance above the tunnel to the centre of the tunnel; $h = H + B$, and H is the vertical distance of the tunnel crown to the ground surface, and B is the radius of the tunnel.

5. Conclusions

This paper provides a brief description of the development and experimental evaluations of the unified critical state model of CASM, in addition to its application to cavity contraction problems and soil tunnelling. The derived analytical cavity contraction solutions in soils modelled by CASM are applied to estimate ground response curves and ground displacements of tunnels in soil under either drained or undrained conditions. Some concluding remarks can be made as follows:

- (1) Extensive experimental evaluations have shown that CASM can give fairly accurate predictions of both drained and undrained stress–strain behaviour of clay and sand. Meanwhile, successful extensions of the basic model CASM, as described in this paper, to other more general cases and material types (Yu, 2006) indicate that this unified critical state framework is very powerful for development and application of constitutive models in geotechnical practise.
- (2) Benefiting from the fact that only a single set of yield and plastic potential functions is required in CASM, this unified critical state model can be easily applied to solving the geotechnical boundary value problems, either analytically or numerically. As a demonstration, the drained and undrained analytical cavity contraction solutions are presented in this paper using CASM to model soil stress–strain behaviour. The derived cavity contraction solutions are shown to be useful for estimating ground response curves and ground displacements of tunnels during their construction.

Conflicts of interest

The authors wish to confirm that there are no known conflicts of interest associated with this publication and there has been no significant financial support for this work that could have influenced its outcome.

Appendix A. Supplementary data

Supplementary data to this article can be found online at <https://doi.org/10.1016/j.jrmge.2018.09.004>.

References

- Ali Rahman Z, Toll D, Gallipoli D. Critical state behaviour of weakly bonded soil in drained state. *Geomechanics and Geoengeering* 2018. <https://doi.org/10.1080/17486025.2018.1454608>.

- Allman MA, Atkinson JH. Mechanical properties of reconstituted Bothkennar soil. *Géotechnique* 1992;42(2):289–301.
- Alonso EE, Gens A, Josa A. A constitutive model for partially saturated soils. *Géotechnique* 1990;40(3):405–30.
- Atkinson JH, Bransby PL. The mechanics of soils, an introduction to critical state soil mechanics. New York: McGraw-Hill; 1977.
- Baud P, Vajdova V, Wong TF. Shear-enhanced compaction and strain localization: Inelastic deformation and constitutive modeling of four porous sandstones. *Journal of Geophysical Research Solid Earth* 2006;111(B12). <https://doi.org/10.1029/2005JB004101>.
- Been K, Jefferies MG. A state parameter for sands. *Géotechnique* 1985;35(2):99–112.
- Been K, Jefferies MG, Hachey J. The critical state of sands. *Géotechnique* 1991;41(3):365–81.
- Bishop AW, Henkel DJ. The measurement of soil properties in the triaxial test. London: Edward Arnold (Publishers) Ltd.; 1957.
- Borja R, Kavazanjian E. A constitutive model for the stress–strain–time behaviour of ‘wet’ clays. *Géotechnique* 1985;35(3):283–98.
- Brady BH, Brown ET. Rock mechanics for underground mining. 2nd ed. London: Chapman & Hall; 1993.
- Brown ET, Bray JW, Ladanyi B, Hoek E. Ground response curves for rock tunnels. *Journal of Geotechnical Engineering* 1983;109(1):15–39.
- Brown ET, Yu HS. A model for the ductile yield of porous rock. *International Journal for Numerical and Analytical Methods in Geomechanics* 1988;12(6):679–88.
- Cao LF, Teh CI, Chang MF. Undrained cavity expansion in modified Cam clay I: Theoretical analysis. *Géotechnique* 2001;51(4):323–34.
- Carranza-Torres C, Fairhurst C. Application of the convergence–confinement method of tunnel design to rock masses that satisfy the Hoek–Brown failure criterion. *Tunnelling and Underground Space Technology* 2000;15(2):187–213.
- Carroll MM. A critical state plasticity theory for porous reservoir rock. *Recent Advances in Mechanics of Structured Continua* 1991;117:1–8.
- Carter JP, Wroth CP, Booker JR. A critical state soil model for cyclic loading. Research Report No. CE 6. St. Lucia, Australia: Department of Civil Engineering, University of Queensland; 1979.
- Carter JP, Booker JR, Yeung SK. Cavity expansion in cohesive frictional soils. *Géotechnique* 1986;36(3):349–58.
- Castro G. Liquefaction of sands. PhD. Thesis. Massachusetts, USA: Harvard University; 1969.
- Castro G, Poulos SJ. Factors affecting liquefaction and cyclic mobility. *Journal of Geotechnical and Geoenvironmental Engineering* 1977;103(6):501–16.
- Chen SL, Abousleiman YN. Exact undrained elasto-plastic solution for cylindrical cavity expansion in modified Cam clay soil. *Géotechnique* 2012;62(5):447–56.
- Chen SL, Abousleiman YN. Exact drained solution for cylindrical cavity expansion in modified Cam clay soil. *Géotechnique* 2013;63(6):510–7.
- Chen SL, Abousleiman YN. Drained and undrained analyses of cylindrical cavity contractions by bounding surface plasticity. *Canadian Geotechnical Journal* 2016;53(9):1398–411.
- Chen SL, Abousleiman YN. Wellbore stability analysis using strain hardening and/or softening plasticity models. *International Journal of Rock Mechanics and Mining Sciences* 2017;93:260–8.
- Chen SL, Liu K. Undrained cylindrical cavity expansion in anisotropic critical state soils. *Géotechnique* 2018. <https://doi.org/10.1680/jgeot.16.P.335>.
- Collins IF, Pender MJ, Yan W. Cavity expansion in sands under drained loading conditions. *International Journal for Numerical and Analytical Methods in Geomechanics* 1992;16(1):3–23.
- Collins IF, Stimpson JR. Similarity solutions for drained and undrained cavity expansions in soils. *Géotechnique* 1994;44(1):21–34.
- Collins IF, Yu HS. Undrained cavity expansions in critical state soils. *International Journal for Numerical and Analytical Methods in Geomechanics* 1996;20(7):489–516.
- Coop MR, Atkinson JH. The mechanics of cemented carbonate sands. *Géotechnique* 1993;43(1):53–67.
- Coop MR, Lee IK. The behaviour of granular soils at elevated stresses. In: Proceedings of Wroth Memorial Symposium. London: Thomas Telford; 1993. p. 186–98.
- Crouch RS, Wolf JP, Dafalias YF. Unified critical-state bounding-surface plasticity model for soil. *Journal of Engineering Mechanics* 1994;120(11):2251–70.
- Cuss R, Rutter E, Holloway R. The application of critical state soil mechanics to the mechanical behaviour of porous sandstones. *International Journal of Rock Mechanics and Mining Sciences* 2003;40(6):847–62.
- Dafalias YF. An anisotropic critical state soil plasticity model. *Mechanics Research Communications* 1986;13(6):341–7.
- Dafalias YF, Herrmann LR. Bounding surface formulation of soil plasticity. In: *Soil Mechanics-transient and Cyclic Loads*. New York, USA: Wiley; 1982. p. 253–82.
- Drucker DC, Gibson RE, Henkel DJ. Soil mechanics and work-hardening theories of plasticity. *Transactions of the American Society of Civil Engineers* 1957;122(1):338–46.
- Elliott GM. An investigation of a yield criterion for porous rock. London, UK: University of London; 1983.
- Franza A. Tunnelling and its effects on piles and piled structures. PhD. Thesis. Nottingham, UK: University of Nottingham; 2017.
- Franza A, Marshall A, Zhou B. Greenfield tunnelling in sands: the effects of soil density and relative depth. *Géotechnique* 2018. <https://doi.org/10.1680/jgeot.17.P.091>.
- Gens A, Potts DM. Critical state models in computational geomechanics. *Engineering Computations* 1988;5(3):178–97.
- Gens A, Nova R. Conceptual basis for a constitutive model for bonded soils and weak rocks. In: *Proceedings of Geotechnical Engineering of Hard Soils-soft Rocks*. Athens, Greece; 1993. p. 485–94.
- Gerogiannopoulos NG, Brown ET. The critical state concept applied to rock. *International Journal of Rock Mechanics and Mining Sciences and Geomechanics Abstracts* 1978;15(1):1–10.
- Gonzalez NA, Arroyo M, Gens A. Identification of bonded clay parameters in SBPM tests: a numerical study. *Soils and Foundations* 2009;49(3):329–40.
- Hoek E, Brown ET. *Underground excavations in rock*. CRC Press; 1980.
- Hu N. On Fabric tensor-based constitutive modelling of granular materials: theory and numerical implementation. PhD. Thesis. Nottingham, UK: University of Nottingham; 2015.
- Hu N, Shang XY, Yu HS. Theoretical analysis of pressure-dependent K_0 for normally consolidated clays using critical state soil models. *International Journal of Geomechanics* 2018;18(3):04017159. [https://doi.org/10.1061/\(ASCE\)GM.1943-5622.0001075](https://doi.org/10.1061/(ASCE)GM.1943-5622.0001075).
- Huang A, Yu HS. *Foundation engineering analysis and design*. New York: Taylor & Francis Group; 2017.
- Jaky J. Pressure in silos. In: *Proceedings of the 2nd International Conference on Soil Mechanics and Foundation Engineering*. Rotterdam: A.A. Balkema; 1948. p. 103–7.
- Jefferies MG. Nor-Sand: a simple critical state model for sand. *Géotechnique* 1993;43(1):91–103.
- Jefferies M, Been K. *Soil liquefaction: A critical state approach*. CRC Press; 2006.
- Khalili N, Habte MA, Valliappan S. A bounding surface plasticity model for cyclic loading of granular soils. *International Journal for Numerical Methods in Engineering* 2005;63(14):1939–60.
- Khong CD. Development and numerical evaluation of unified critical state models. PhD. Thesis. Nottingham, UK: University of Nottingham; 2004.
- Klotz EU, Coop MR. On the identification of critical state lines for sands. *Geotechnical Testing Journal* 2002;25(3):289–302.
- Kutter B, Sathialingam N. Elastic-viscoplastic modelling of the rate-dependent behaviour of clays. *Géotechnique* 1992;42(3):427–41.
- Lade PV, Yamamoto JA. Undrained sand behavior in axisymmetric tests at high pressures. *Journal of Geotechnical Engineering* 1996;122(2):120–9.
- Lee KL, Seed HB. Drained strength characteristics of sands. *Journal of the Soil Mechanics and Foundations Division* 1967;93(6):117–41.
- Leroueil S, Vaughan PR. The general and congruent effects of structure in natural soils and weak rocks. *Géotechnique* 1990;40(3):467–88.
- Li L, Li J, Sun DA. Anisotropically elasto-plastic solution to undrained cylindrical cavity expansion in K_0 -consolidated clay. *Computers and Geotechnics* 2016;73:83–90.
- Liu MD, Carter JP. A structured Cam Clay model. *Canadian Geotechnical Journal* 2002;39(6):1313–32.
- Mair RJ. Centrifugal modelling of tunnel construction in soft clay. PhD. Thesis. Cambridge, UK: Cambridge University; 1979.
- Mair RJ, Taylor RN. Prediction of clay behaviour around tunnels using plasticity solutions, predictive soil mechanics. In: *Proceedings of the Wroth Memorial Symposium*. Oxford, UK: Thomas Telford; 1993. p. 449–63.
- Matsuoka H, Nakai T. Stress-deformation and strength characteristics of soil under three different principal stresses. In: *Proceedings of the Japan Society of Civil Engineers*. Japan: JSCCE; 1974. p. 59–70. https://doi.org/10.2208/jsccej1969.1974.232_59.
- McDowell GR. A simple non-associated flow model for sand. *Granular Matter* 2002;4(2):65–9.
- McDowell GR, Hau KW. A simple non-associated three surface kinematic hardening model. *Géotechnique* 2003;53(4):433–7.
- Mita K, Dasari G, Lo K. Performance of a three-dimensional Hvorslev–modified Cam clay model for overconsolidated clay. *International Journal of Geomechanics* 2004;4(4):296–309.
- Mo PQ, Yu HS. Undrained cavity-contraction analysis for prediction of soil behavior around tunnels. *International Journal of Geomechanics* 2017a;17(5):04016121 (1–10). [https://doi.org/10.1061/\(ASCE\)GM.1943-5622.0000816](https://doi.org/10.1061/(ASCE)GM.1943-5622.0000816).
- Mo PQ, Yu HS. Undrained cavity expansion analysis with a unified state parameter model for clay and sand. *Géotechnique* 2017b;67(6):503–15.
- Mo PQ, Yu HS. Drained cavity expansion analysis with a unified state parameter model for clay and sand. *Canadian Geotechnical Journal* 2018;55(7):1029–40.
- Navarro V, Alonso J, Calvo B, Sánchez J. A constitutive model for porous rock including effects of bond strength degradation and partial saturation. *International Journal of Rock Mechanics and Mining Sciences* 2010;47(8):1330–8.
- Naylor DJ. A continuous plasticity version of the critical state model. *International Journal for Numerical Methods in Engineering* 1985;21(7):1187–204.
- Nova R, Wood DM. A constitutive model for sand in triaxial compression. *International Journal for Numerical and Analytical Methods in Geomechanics* 1979;3(3):255–78.
- Novello E, Johnston L. Geotechnical materials and the critical state. *Géotechnique* 1995;45(2):223–35.
- Ohmaki S. Stress-strain behaviour of anisotropically, normally consolidated cohesive soil. In: *Proceeding of 1st International Symposium on Numerical Methods of Geomechanics*. Zurich; 1982. p. 250–69.
- Ohta H, Wroth CP. Anisotropy and stress reorientation in clay under load. In: *Proceeding of 2nd International Conference on Numerical Methods in Geomechanics*. Blacksburg; 1976. p. 319–28.
- Park KH. Similarity solution for a spherical or circular opening in elastic-strain softening rock mass. *International Journal of Rock Mechanics and Mining Sciences* 2014;71:151–9.

- Parry RHG. Strength and deformation of clay. PhD. Thesis. London, UK: University of London; 1956.
- Parry RHG. Correspondence on 'On the yielding of soils'. *Géotechnique* 1958;8(4):183–6.
- Pender MJ. A model for the behaviour of overconsolidated soil. *Géotechnique* 1978;28(1):1–25.
- Pestana JM, Whittle AJ. Formulation of a unified constitutive model for clays and sands. *International Journal for Numerical and Analytical Methods in Geomechanics* 1999;23(12):1215–43.
- Poulos SJ. The steady state of deformation. *Journal of the Geotechnical Engineering Division* 1981;107(5):553–62.
- Price AM, Farmer IW. The Hvorslev surface in rock deformation. *International Journal of Rock Mechanics and Mining Sciences and Geomechanics Abstracts* 1981;18(3):229–34.
- Randolph MF, Wroth CP. An analytical solution for the consolidation around a driven pile. *International Journal for Numerical and Analytical Methods in Geomechanics* 1979;3(3):217–29.
- Roscoe KH, Schofield AN, Wroth CP. On the yielding of soils. *Géotechnique* 1958;8(1):22–53.
- Roscoe KH, Schofield AN. Mechanical behaviour of an idealized 'wet' clay. In: *Proceeding of the 3rd European Conference Soil Mechanics and Foundation Engineering*. Wiesbaden; 1963. p. 47–54.
- Roscoe KH, Burland JB. On the generalized stress-strain behaviour of wet clay. In: *Heymann G, Leckie FA, editors. Engineering Plasticity*. Cambridge, UK: Cambridge University Press; 1968. p. 535–609.
- Rowe PW. The stress-dilatancy relation for static equilibrium of an assembly of particles in contact. In: *Proceedings of the Royal Society of London A: Mathematical, Physical and Engineering Sciences*. London: The Royal Society; 1962. p. 500–27.
- Russell AR, Khalili N. Drained cavity expansion in sands exhibiting particle crushing. *International Journal for Numerical and Analytical Methods in Geomechanics* 2002;26(4):323–40.
- Rutter EH, Glover CT. The deformation of porous sandstones; are Byerlee friction and the critical state line equivalent? *Journal of Structural Geology* 2012;44:129–40.
- Salgado R, Mitchell JK, Jamiolkowski M. Cavity expansion and penetration resistance in sand. *Journal of Geotechnical and Geoenvironmental Engineering* 1997;123(4):344–54.
- Salgado R, Randolph MF. Analysis of cavity expansion in sand. *International Journal of Geomechanics* 2001;1(2):175–92.
- Schofield AN, Wroth CP. *Critical state soil mechanics*. London: McGraw-Hill; 1968.
- Sharan SK. Analytical solutions for stresses and displacements around a circular opening in a generalized Hoek–Brown rock. *International Journal of Rock Mechanics and Mining Sciences* 2008;45(1):78–85.
- Sheng D, Sloan SW, Yu HS. Aspects of finite element implementation of critical state models. *Computational Mechanics* 2000;26(2):185–96.
- Sladen JA, D'hollander RD, Krahn J. The liquefaction of sands, a collapse surface approach. *Canadian Geotechnical Journal* 1985;22(4):564–78.
- Stroud M. The behaviour of sand at low stress levels in the simple shear apparatus. PhD. Thesis. Cambridge, UK: University of Cambridge; 1971.
- Toll D, Ong B. Critical-state parameters for an unsaturated residual sandy clay. *Géotechnique* 2003;53(1):93–103.
- Verdugo R, Ishihara K. The steady state of sandy soils. *Soils and Foundations* 1996;36(2):81–91.
- Verruijt A, Booker JR. Surface settlements due to deformation of a tunnel in an elastic half plane. *Géotechnique* 1996;46(4):753–6.
- Vesic AS, Clough GW. Behavior of granular materials under high stresses. *Journal of the Soil Mechanics and Foundations Division* 1968;94(3):661–88.
- Vesic AS. Expansion of cavities in infinite soil mass. *Journal of Soil Mechanics and Foundations Division* 1972;98(SM3):265–90.
- Vrakas A. Analysis of ground response and ground-support interaction in tunnelling considering large deformations. PhD. Thesis. Zurich: ETH Zurich; 2016a.
- Vrakas A. A rigorous semi-analytical solution for undrained cylindrical cavity expansion in critical state soils. *International Journal for Numerical and Analytical Methods in Geomechanics* 2016b;40(15):2137–60.
- Vrakas A, Dong W, Anagnostou G. Elastic deformation modulus for estimating convergence when tunnelling through squeezing ground. *Géotechnique* 2017;68(8):713–28.
- Wang J. The stress-strain and strength characteristics of Portaway sand. PhD. Thesis. Nottingham, UK: University of Nottingham; 2005.
- Whittle AJ. Evaluation of a constitutive model for overconsolidated clays. *Géotechnique* 1993;43(2):289–313.
- Wong TF, David C, Zhu WL. The transition from brittle faulting to cataclastic flow in porous sandstones: Mechanical deformation. *Journal of Geophysical Research: Solid Earth* 1997;102(B2):3009–25.
- Wood DM. *Soil behaviour and critical state soil mechanics*. Cambridge, UK: Cambridge University Press; 1990.
- Wroth CP, Bassett R. A stress-strain relationship for the shearing behaviour of a sand. *Géotechnique* 1965;15(1):32–56.
- Wroth CP, Houlsby GT. *Soil mechanics: property characterization and analysis procedures*. Rotterdam, the Netherlands: A.A. Balkema; 1985. p. 1–55.
- Yang J. Non-uniqueness of flow liquefaction line for loose sand. *Géotechnique* 2002;52(10):757–60.
- Yang J, Li XS. State-dependent strength of sands from the perspective of unified modeling. *Journal of Geotechnical and Geoenvironmental Engineering* 2004;130(2):186–98.
- Yao YP, Sun DA, Matsuoka H. A unified constitutive model for both clay and sand with hardening parameter independent on stress path. *Computers and Geotechnics* 2008;35(2):210–22.
- Yu HS, Houlsby GT. Finite cavity expansion in dilatant soils: Loading analysis. *Géotechnique* 1991;41(2):173–83.
- Yu HS. State parameter from self-boring pressuremeter tests in sand. *Journal of Geotechnical Engineering* 1994;120(12):2118–35.
- Yu HS. A unified state parameter model for clay and sand. *Civil Engineering Research Report No. 112.08.1995*. NSW, Australia: University of Newcastle; 1995.
- Yu HS. CASM: A unified state parameter model for clay and sand. *International Journal for Numerical and Analytical Methods in Geomechanics* 1998;22(8):621–53.
- Yu HS, Rowe RK. Plasticity solutions for soil behaviour around contracting cavities and tunnels. *International Journal for Numerical and Analytical Methods in Geomechanics* 1999;23(12):1245–79.
- Yu HS. Cavity expansion methods in geomechanics. The Netherlands: Kluwer Academic Publishers; 2000.
- Yu HS, Khong CD. Application of a unified plasticity model in finite element analysis. In: *Proceedings of the 3rd International Symposium on 3D Finite Element for Pavement Analysis, Design and Research*. Amsterdam: A.A. Balkema; 2002. p. 253–67.
- Yu HS, Khong CD, Wang J, Zhang G. Experimental evaluation and extension of a simple critical state model for sand. *Granular Matter* 2005;7(4):213–25.
- Yu HS. *Plasticity and geotechnics*. New York, USA: Springer; 2006.
- Yu HS, Khong CD, Wang J. A unified plasticity model for cyclic behaviour of clay and sand. *Mechanics Research Communications* 2007a;34(2):97–114.
- Yu HS, Tan SM, Schnaid F. A critical state framework for modelling bonded geomaterials. *Geomechanics and Geoenvironmental Engineering* 2007b;2(1):61–74.
- Zhou B. Tunnelling-induced ground displacements in sand. PhD. Thesis. Nottingham, UK: University of Nottingham; 2015.
- Zhou C, Ng CWV. A thermomechanical model for saturated soil at small and large strains. *Canadian Geotechnical Journal* 2015;52(8):1101–10.
- Zhou H, Kong G, Liu H, Laloui L. Similarity solution for cavity expansion in thermoplastic soil. *International Journal for Numerical and Analytical Methods in Geomechanics* 2018;42(2):274–94.
- Zhuang PZ, Yu HS, Hu N. Size-dependent finite strain analysis of cavity expansion in frictional materials. *International Journal of Solids and Structures* 2018;150:282–94.
- Zienkiewicz OC, Naylor DJ. *Finite element studies of soils and porous media*. In: *Oden JT, de Arantes ER, editors. Lectures on Finite Elements in Continuum Mechanics*. Huntsville, AL, USA: University of Alabama in Huntsville Press; 1973. p. 459–93.
- Zienkiewicz OC, Pande GN. Some useful forms of isotropic yield surfaces for soil and rock mechanics. In: *Finite Element in Geomechanics* 1977. Wiley; 1977. p. 179–90.
- Zytynski M, Randolph MF, Nova R, Wroth CP. On modelling the unloading-reloading behaviour of soils. *International Journal for Numerical and Analytical Methods in Geomechanics* 1978;2(1):87–93.



Professor Hai-Sui Yu is Professor of Geotechnical Engineering and Deputy Vice-Chancellor at the University of Leeds, UK, and was elected a Fellow of the Royal Academy of Engineering in 2011. Professor Yu worked at the University of Newcastle, Australia from 1990 to 2000 before taking up the foundation Professorship of Geotechnical Engineering at the University of Nottingham in 2001, where he founded the Nottingham Centre for Geomechanics. He also served as Head of the School of Civil Engineering, Dean of the Faculty of Engineering, and Pro-Vice-Chancellor there. Professor Yu's main research activities have focused on theoretical and computational geomechanics, constitutive modelling, in situ soil testing, and pavement & railway geotechnics. Professor Yu is very active in professional activities and services and is the founding Editor-in-Chief of *Geomechanics and Geoenvironmental Engineering*. He has been awarded many international medals and prizes for his research work, which include the British Geotechnical Association Medal for 2015, the Outstanding Contributions Medal of the International Association for Computer Methods and Advances in Geomechanics (IACMAG) in 2014, the Chandra Desai Medal of IACMAG in 2008, the first James K Mitchell Lecture of the International Society for Soil Mechanics and Geotechnical Engineering in 2004, Shamsher Prakash Foundation's Research Award in 2003, the Institution of Civil Engineers' highest research paper award, the Telford Medal, in 2000, and Australian Geomechanics Society's Trollope Medal in 1998.